Environment International 184 (2024) 108471

Contents lists available at ScienceDirect

Environment International

journal homepage: www.elsevier.com/locate/envint

Full length article

# The blue light hazard and its use on the evaluation of photochemical risk for domestic lighting. An *in vivo* study

Anaïs Françon [a], Francine Behar-Cohen [a,b], Alicia Torriglia [a,*]

[a] Centre de Recherche des Cordeliers, INSERM UMRS 1138, Université Paris Cité, Sorbonne Université. Team: Physiopathology of Ocular Diseases: Therapeutic Innovations. 15, rue de l'école de Médecine, 75006 Paris, France
[b] Assistance Publique, Hôpitaux de Paris, Hôpital Cochin, Ophtalmopole, 27, rue du Faubourg Saint-Jacques, 75014 Paris, France

ARTICLE INFO

*Keywords:*
Phototoxicity
Light
Retina
Blue Light Hazard
Apoptosis
Inflammation

ABSTRACT

*Background:* Nowadays artificial light highly increases human exposure to light leading to circadian rhythm and sleep perturbations. Moreover, excessive exposure of ocular structures to photons can induce irreversible retinal damage. Meta-analyses showed that sunlight exposure influences the age of onset and the progression of Age-related macular degeneration (AMD), the leading cause of blindness in people over fifty-year old. Currently, the blue-light hazard (BLH) curve is used in the evaluation of the phototoxicity of a light source for domestic lighting regulations.

*Objectives:* Here, we analyze the phototoxicity threshold in rats and investigate the role played by the light spectrum, assessing the relevance of the use of the BLH-weighting to define phototoxicity.

*Methods:* We exposed albino rats to increasing doses of blue and white light, or to lights of different colors to evaluate the impact of each component of the white light spectrum on phototoxicity. Cellular mechanisms of cell death and cellular stress induced by light were analyzed.

*Results:* Our results show that the phototoxicity threshold currently accepted for rats is overestimated by a factor of 50 when considering blue light and by a factor of 550 concerning white light. This is the result of the toxicity induced by green light that increases white light toxicity by promoting an inflammatory response. The content of green in white light induces 8 fold more invasion of macrophages in the retina than the content of blue light. Moreover, the use of BLH-weighting does not evaluate the amount of red radiations contained in white light that mitigates damage by inhibiting the nuclear translocation of L-DNase II and reducing by 33% the number of TUNEL-positive cells.

*Discussion:* These findings question the current methods to determine the phototoxicity of a light source and show the necessity to take into account the entire emission spectrum. As current human phototoxicity thresholds were estimated with the same methods used for rats, our results suggest that they might need to be reconsidered.

## 1. Introduction

Although the eye is protected from the oxidant effect of light by complex and powerful antioxidant systems, excessive exposure of ocular structures to photons can induce non-reversible tissue damage. The retina, which ensures phototransduction, is particularly vulnerable to damage when exposed to acute high light doses as shown by retinal injuries reported in human after staring at solar eclipses or at surgical microscopes (Gosling et al., 2016; Liang et al., 2017). Moreover, although the exact role of sunlight in Age-related macular degeneration (AMD), the leading cause of blindness in people over fifty-year old, is more complex to determine and is matter of debate, *meta*-analyses showed that sunlight exposure history influences the age of onset and the progression of the disease (Oddone et al., 2019; Schick et al., 2016; Sui et al., 2013; Zhou et al., 2018).

Nowadays, increasing exposure to artificial light during the day and night is added to the natural sunlight exposure (Contín et al., 2016). This became quantitatively important since the development of the LED (light emitting diodes) technology. Most LED used for domestic lighting produce a white light by exciting a blue diode covered by a yellow phosphor layer. Therefore, these LED emit a spectrally imbalanced light characterized by a peak in the blue region of the visible spectrum, at

* Corresponding author.
*E-mail address:* alicia.torriglia@inserm.fr (A. Torriglia).

https://doi.org/10.1016/j.envint.2024.108471
Received 22 August 2023; Received in revised form 16 January 2024; Accepted 30 January 2024
Available online 2 February 2024

about 450 nm, a green-yellow peak, and a weak emission in the red part of the spectrum. Their spectrum is, therefore, very different from the one produced by incandescent devices formerly used, which are rich in red wavelengths and poor in blue wavelengths.

This leads to the investigation of the effects of blue light on health and to the description of two important parts of the blue radiation. First, wavelengths between 470 and 490 nm activate melanopsin, a non-visual pigment involved in circadian rhythm synchronization (defined by the melanopic curve (Brown, 2020)), and trigger sleep disruption and many health effects (Hatori et al., 2017). Then, the range between 400 and 490 nm (defined by the phototoxic curve (Legierski and Michałek, 2018)) mediates photochemical damage to the retina (Court, 2012). This last effect will be studied in this paper.

Light-induced photochemical damage to the retina (Noell et al., 1966) leads to the death of photoreceptors (Remé et al., 2000) and retinal pigment epithelial (RPE) cells (Jaadane et al., 2017), as demonstrated in various animal models. Exposure to white LED light triggers oxidative stress (Benedetto and Contin, 2019), apoptosis and necroptosis of photoreceptors (Jaadane et al., 2015; Shang et al., 2014), as well as RPE damage (Jaadane et al., 2017).

For Human retina, limit exposure values (LEV) for domestic lighting devices have been established based on the action spectrum curves (van Norren and Gorgels, 2011). These curves show that the blue light, which is the most energetic part of the visible spectrum, is the most phototoxic with a retinal threshold dose at 445 nm of 22 J/cm$^2$ for primates and 11 J/cm$^2$ for rodents (rats, mice, squirrels). The values obtained from primates were used to establish the current lighting regulations, which are based on the energetic weighting of polychromatic light by the so-called Blue Light Hazard (BLH) curve. The BLH of a lighting source is evaluated by the action spectrum curve B(λ), corresponding to a weighting curve picking at 445 nm. So that, according to the NF EN 62471 regulation, a lighting device is labeled at no risk if, after 10,000 s of exposure the BLH-weighted retinal dose is under 2.2 J/cm$^2$ (the safety limit or limit exposure value (LEV) corresponding to 1/10 of the basic restriction value of 22 J/cm$^2$ described above). Nowadays, most of the commercially available LED fall into this group. Thus, under normal use and according to these criteria, they are safe for the retina (Bullough et al., 2019).

As stated in the paragraph above the light exposure magnitude used in the normative is the retinal dose. For this reason, and in order to give more precise information, we use the retinal dose to measure light exposure in this paper. The retinal dose represents the amount of energy that reaches the retina. This includes the time of exposure but also the retinal illumination which is calculated by taking into account the geometry and the absorption of the rat eye. This is an important point because it is currently believed that the retina of albino animals is intrinsically more sensitive to light than the retina of pigmented animals. However, the amount of light that reaches the retina is different and thus, pigmented and albino animals are not receiving the same retinal dose under the same lighting conditions. This is why in the action spectrum curves of Van Norren (van Norren and Gorgels, 2011), it can be seen that albino and pigmented rats have the same sensitivity to light.

This study focuses on the relevance of the current LEV. By exposing Wistar rats to blue and white light, we give a new assessment of phototoxicity thresholds for this animal model. We also focus on the role of the spectral composition of the light source in its toxicity, by comparing the toxicity of blue, green, white and red light, challenging the use of the BLH weighting in the evaluation of phototoxicity of lighting devices.

## 2. Methods

### 2.1. Animals

Three-week old male albino Wistar rats were purchased from Charles Rivers, left in the animal facility for 3 weeks for acclimation and exposed to light at 6 weeks old. All procedures were performed according to the animal use and care committee of the Ecole Nationale Vétérinaire d'Alfort (Apafis #21910-2019090612065253v6).

### 2.2. Light source

The light exposure devices were manufactured and designed by the CSTB (Centre Scientifique et Technique du Bâtiment Saint Martin d'Heres, France) as described in Jaadane et al., 2015 (Jaadane et al., 2015). The devices are composed of 10 LED disposed to evenly lighten the rats from the top. LED used in this study were white LED (PC-LED phosphor type) (CT: 2700 K, Xanlite XXX Evolution 5 W), blue LED (450 nm, Cree royal blue), green LED (507 nm, Nichia NCSE 119A blue-green), and red LED (630 nm, Qasim LED type 3528). The different light sources were evaluated (peak of emission, integrated irradiance, CT, etc) using a Konica Minolta CL70 F CR I spectroradiometer. The spectra of the different lights used in this study are seen in Fig. 1.

### 2.3. Light exposure

Wistar rats were individually exposed to LED light at 9AM. The exposure time varied according to the different retinal doses (as calculated below) indicated in each figure. The rats were then kept in the dark for a period of 26 h before sacrifice. This time point corresponds to the peak of photoreceptor cell death after an exposure to white light, as shown in supplementary Fig. 1. In the case of rats being sacrificed one week after exposure, rats returned to the animal facility in normal lighting conditions right after light exposure. Control animals stayed in the animal facility at normal lighting conditions.

### 2.4. Retinal dose

The dosimetry approach was developed in Jaadane et al., 2015 (Jaadane et al., 2015).

In their seminar paper, Ham et al. show that retinal light damage depends on the retinal dose of light received by the retina, which depends on the amount of light reaching the retina (retinal irradiance) and the time of exposure (Ham et al., 1982), calculated as follows:

$$D_r = tE_r[J.m^{-2}]$$

where $D_r$ is the retinal dose, $t$ is the exposure time in seconds, and $E_r$ is the integrated spectral retinal irradiance (total light irradiance).

The total retinal irradiance was obtained using the following mathematical approximation:

$$E_{\lambda,r} = \tau E_{\lambda,c} d_p^2 / 8f^2 [W.m^{-2}.nm^{-1}]$$

where $E_{\lambda,r}$ represents the total retinal illuminance, τ the transmittance of the ocular media, $E_{\lambda,c}$ the integrated spectral irradiance of the incident light (including all the wavelengths of the incident light), $d$ the diameter of the pupil, $f$ the focal eye length.

Blue light hazard (BLH) weighting:

The "Blue Light Hazard" refers to a specific photochemical induced damage to the retina (photoretinitis) and not to the disruption of the circadian rhythm, which is not studied, nor evaluated in this paper. In the evaluation of domestic lighting, this function allows the evaluation of the blue light content. The weighting function, also called BLH function or B(λ) function, is defined over the 300–700 nm range but presents a strong responsive peak at 445 nm (see ICNIRP guidelines (International Commission on Non-Ionizing Radiation Protection, 2013)). As it is done in current regulations (see IEC 62471) we used the B (λ) curve to calculate the BHL-weighted dose of the incident light.

A summary of the retinal doses used in this paper is displayed in Table 1.

The physical characteristics of the used LED and the exposure times according to the retinal doses to obtain are displayed in Table 2.

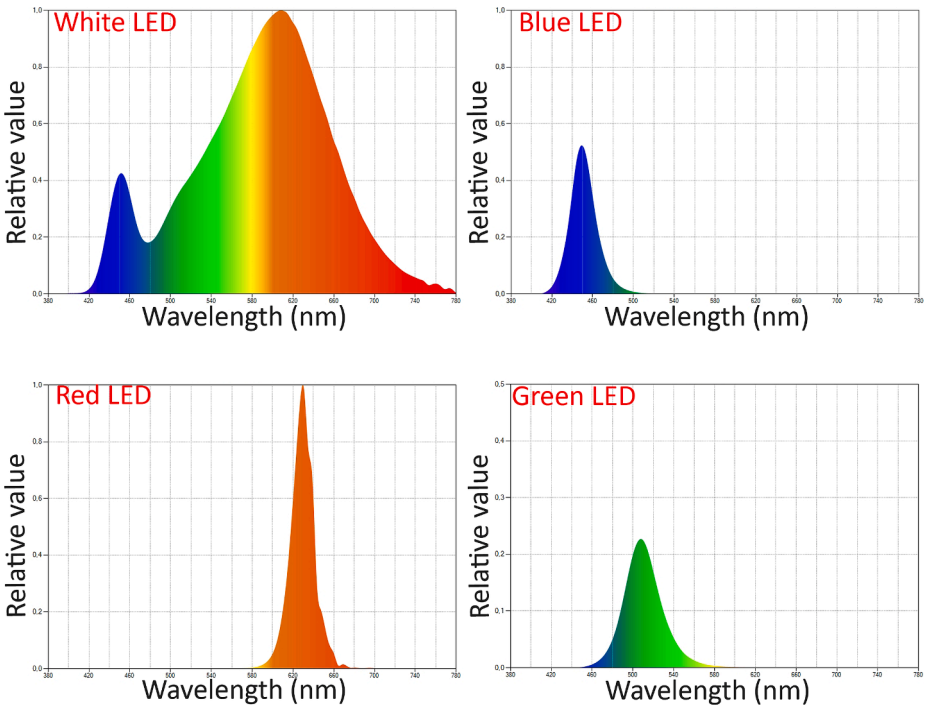


**Fig. 1.** Spectra of the LED used in this study.

**Table 1**
Summary of the retinal doses used for blue and white LED (in J/cm$^2$).

| Blue LED | White LED | |
|---|---|---|
| Total dose (=BLH-weighted dose) | Total dose | Corresponding BLH-weighted dose |
| 0.1 | 0.1 | 0.01 |
| 0.2 | 0.2 | 0.02 |
| 0.5 | 0.5 | 0.05 |
| 0.9 | 0.9 | 0.09 |
| | 2.0 | 0.2 |

**Table 2**
Characteristics of the LED and exposure times used in this study.

| LED | Corneal irradiance | Exposure time |
|---|---|---|
| Blue (449 nm) | 0.9 mW/cm$^2$ (BLH 0.9 mW/cm$^2$) | 30 min for 0.1 J/cm$^2$ (BLH or total dose) to 4 h for 0.9 J/cm$^2$(BLH or total dose) |
| White (2 700 K) | 3.14 mW/cm$^2$ (BLH 0.3 mW/cm$^2$) | 1 h for 0.1 J/cm$^2$ (BLH 0.01 J/cm$^2$) to 16 h45 min for 2 J/cm$^2$ (BLH 0.2 J/cm$^2$) |
| Red (630 nm) | 0.05 mW/cm$^2$ (BLH 7.8e10-5 mW/cm$^2$) | 8 h30 for 0.1 J/cm$^2$ (BLH 0.2 mJ/cm$^2$) |
| White + Red | 3.2 mW/cm$^2$ (BLH 0.3 mW/cm$^2$) | 8 h30 for 1.0 J/cm$^2$ (BLH 0.09 J/cm$^2$) |
| Green (508 nm) | 0.6 mW/cm$^2$ (BLH 0.07 mW/cm$^2$) | 4 h15 for 0.8 J/cm$^2$ |

### 2.5. Tissue preparation

Rats were sacrificed with a lethal intra-peritoneal dose of pentobarbital. Eyes were immediately tagged with a stitch for orientation and enucleated. They were then fixed in 4 % paraformaldehyde (PFA) in phosphate buffered saline (PBS) for 2 h, washed for one hour in PBS and embedded in optimal cutting-temperature compound (OCT, TissueTek Sakura). Ten micrometer cryosections of the eyes, containing the optic nerve, were obtained using a Leica CM3050S cryostat. Alternatively, the neural retina of some eyes was dissected for western blot purposes, while the RPE was prepared as flat mounts and fixed for 15 min with 4 % PFA.

### 2.6. Protein extraction

Neural retinas were homogenized with 20 % weight–volume of M−PER Mammalian Protein Extraction Reagent (Thermo Scientific, Illkirch, France), left for 15 min in ice before centrifugation at 4 °C, 15,000 g for 5 min. The supernatant was collected and stored at −20 °C. Protein concentration was measured using the bicinchoninic acid (BCA)$^{TM}$ Protein Assay Kit (Thermo Scientific, Illkirch, France), according to the manufacturer's instructions.

### 2.7. Western blot

For western blot analysis, protein samples were prepared with Laemmli sample buffer (10 % Glycerol, 2 % SDS, 100 mM Dithiothreitol, 62.5 mM Tris, Bromophenol blue) containing 20 µg of proteins per well and separated in a Bolt$^{TM}$ 4–12 % Bis-Tris Plus gel (Thermo Scientific, Illkirch, France, NW04125BOX). Proteins were transferred to nitrocellulose membrane (Protan ®, Whatman ®, GE Healthcare, Versailles, France). Membranes were saturated in 5 % dry skimmed milk in PBS one hour at room temperature, washed and incubated with the primary antibody (1:1000 in PBS with 0.5 % dry skimmed milk and 0.1 % Tween) for two hours (Table 3). Then membranes were incubated with a secondary HorseRadish Peroxidase (HRP) tagged antibody (1:5000 in PBS with 0.1 % Tween) for one hour. SuperSignal$^{TM}$ West Pico PLUS (Thermo Scientific, Illkirch, France, 34578) was used as HRP substrate and chemiluminescence was captured with the iBright$^{TM}$ CL1500 Imaging System (Thermo Scientific, Illkirch, France). The measurement of the integrated density of the specific band for each protein of interest was normalized over the one of the glyceraldehyde-3-phosphate dehydrogenase (GAPDH) protein. The results show the ratio between the value of the protein of interest and the one of the corresponding control condition (non-exposed rats) in arbitrary units (AU).

### 2.8. Immunolabeling

Immunofluorescent staining was performed on cryosections of the eye and flat mounts of the RPE. Cryosections were rinsed once with PBS

containing $Ca^{2+}$ and $Mg^{2+}$. Cryosections and flat mounts were fixed for 15 min with 4 % PFA, washed with PBS and permeabilized with 0.3 % Triton X-100 for 30 min at room temperature. They were then washed and incubated with the primary antibody (1:100 in PBS with 1 % BSA) (Table 3) for one hour. Both samples were then incubated with the secondary tagged antibody (1:200 in PBS with 1 % BSA) for one hour. Finally, cryosections and flat mounts were incubated for 5 min with DAPI (4′,6 diamidino-2-phenylindole) (1:1000 in PBS). This was followed, for flat mounts, by a 5-min incubation with AlexaFluor 594-phalloidin (Santa Cruz, 1:1000 in PBS with 1 % BSA). Labeled samples were mounted with Fluoromount (Sigma).

### 2.9. TUNEL assay

Cryosections of the eye were fixed for 15 min with 4 % PFA washed with PBS and permeabilized with 0.3 % Triton X-100 for 15 min at room temperature. A dephosphorylating step was performed using the Calf Intestinal Alkaline Phosphatase (CIAP) 10U by section for 30 min at 37 °C (Lebon et al., 2015). Then cryosections were incubated with the TUNEL mix for one hour at 37 °C (Roche TUNEL kit, Sigma), according to the manufacturer's instructions and then for 5 min with DAPI (1:1000 in PBS) before mounting with PBS:glycerol (1:1, v/v).

### 2.10. Imaging

Images of fluorescent staining and TUNEL staining were obtained using an Olympus BX51 microscope (20x objective). Flat mounts and LEI/L-DNase II staining on retina sections were imaged with a confocal microscope (Zeiss LSM 710) using a 40x or 63x oil immersion objective.

### 2.11. Statistical analysis

For statistical analysis, significance was evaluated using the Mann-Whitney test or the Kruskal-Wallis test, followed by the Dunn's multiple comparison post-test. Results are considered significant when the p-value is inferior to 0.05. *$p < 0.05$, **$p < 0.01$, ***$p < 0.001$. All graphs represent the median of the measures. n corresponds to the number of eyes used per conditions and can include the two eyes of the same rat.

## 3. Results

### 3.1. Phototoxicity of blue light

Previous work (Jaadane et al., 2020) suggested that the phototoxicity threshold for rats was overestimated. Here, we first estimated the phototoxicity threshold for blue wavelengths. We used a single acute exposure to blue light at the retinal doses calculated as explained above (see 2.4) and by using the integrated spectrum of the incident light (Fig. 2). The light-induced damage was evaluated 26 h after exposure (setting experiments showed that the number of TUNEL-positive cells was maximal at this time point).

We detected a significant number of apoptotic cells all along the outer nuclear layer (ONL) at retinal doses of 0.5 J/cm$^2$ (median number of TUNEL-positive cells per retina for NE = 4.00, and for B 0.5 J/cm$^2$ = 449.5) (Fig. 2A, B). The inflammatory response was evaluated by immunostaining of the ionized calcium binding adaptor molecule 1 (IBA1), expressed by microglia and macrophages. A significant infiltration of IBA1-positive cells in the inner and outer nuclear layers started at a retinal dose of 0.2 J/cm$^2$ (Fig. 2C, D) (median increasing from 0.001 to 0.01 IBA1-positive cells /μm), suggesting that some damage was in progress.

The impact of blue light exposure on the RPE was also investigated. The sealing of the outer blood-retinal barrier (OBRB) was evaluated by anti-albumin staining. It revealed some leakage of the OBRB at 0,9 J/cm$^2$ (Fig. 2E, arrow). However, accumulations of albumin in the RPE of exposed rats were seen at lower doses, suggesting an overload of the RPE cells ahead of the OBRB demise (Naylor et al., 2019) (Fig. 2E). The phalloidin staining on RPE flat mounts highlighted the appearance of giant multinucleated cells (Fig. 2F).

We have previously shown (Jaadane et al., 2020, 2015) that exposure to higher doses of light triggers caspase-independent apoptosis involving the leukocyte elastase inhibitor (LEI)/L-DNase II pathway, and necrosis involving increased expression of receptor-interacting protein 3 (RIP3). Western blot analysis showed an increase of LEI and L-DNase II at a retinal dose of 0.9 J/cm$^2$ (Fig. 2G). No sign of RIP3 activation was seen neither by increase of the protein expression, nor by its cleavage (Fig. 2H).

In order to verify that the changes seen at 0.5 J/cm$^2$ effectively led to a permanent alteration of the retina, retinas were analyzed one week after exposure. A significant loss of photoreceptors (Fig. 3) was found (thinner ONL) (Fig. 3A) localized at the superior pole of the retina, close to the optic nerve, along with a significant decrease of the number of photoreceptors (from 4.198 to 3.396 cells/μm) (Fig. 3B). The impact of blue light exposure on cones and rods was evaluated using an anti-cone arrestin and an anti-rhodopsin staining. Although the number of cones in the superior part of the retina stayed unchanged (0.07918 and 0.07641 cones/μm) (Fig. 3C), the morphology of both cone and rod segments was altered (Fig. 3D) with a significant decrease of the rod segment length (11.64 μm for NE and 8.370 μm for blue light) (Fig. 3E) and cone segment size (31.92 μm$^2$ for NE and 23.70 μm$^2$ for blue light) (Fig. 3F).

**Table 3**
List of the used antibodies.

| Antibody | Source | Application | Reference |
|---|---|---|---|
| Albumin | Goat | IF | Sigma (A1151) |
| Rhodopsin (Rho4D2) | Mouse | WB/IF | Millipore (MABN15) |
| Cone arrestin | Rabbit | IF | Millipore (ab15282) |
| GFAP | Rabbit | WB/IF | Dako (Z0334) |
| P62/SQSTM1 | Rabbit | WB | Sigma (P0067) |
| IBA1 | Rabbit | IF | Wako (019–19741) |
| LEI/L-DNase II | Rabbit | WB/IF | Home made |
| RIP3 | Rabbit | WB | Sigma (PRS2283) |
| HSP70 | Mouse | WB | BD biosciences (610607) |

WB: Western blot; IF: Immunofluorescence.

### 3.2. Phototoxicity of white light

The current LEV used for domestic lighting assumes that the blue part of the spectrum is responsible for retinal damage. So that, the phototoxicity of white light is evaluated according to its content in blue light by applying the BLH weighting function (B(λ)). Animals were then exposed to a warm white LED (2700 K) according to the BLH-weighted retinal doses, ranging from 0.01 J/cm$^2$ BLH to 0.2 J/cm$^2$ BLH, to match the doses used in Fig. 2 for blue LED (the blue component of this light represents about 10 % of the total spectrum so, the BLH-weighted retinal dose corresponds to one tenth of the total retinal dose). Note that the total retinal dose was calculated by using the integrated spectrum after weighting and not just the peak of emission. TUNEL staining showed that white LED induced a significant photoreceptor cell loss at a retinal dose of 0.05 J/cm$^2$ BLH, the median number of TUNEL-positive cells rising form 4.00 for non-exposed retinas to 674 for retinas exposed to white light at 0.05 J/cm$^2$ BLH (Fig. 4A, 4B). This also induced an inflammatory response with invasion of microglia in the ONL and inner nuclear layer (Fig. 4C). These were statistically significant at a dose of 0.05 J/cm$^2$ BLH (0.001 and 0.01 cells/μm non exposed vs exposed retinas) (Fig. 4D).

Focusing on the RPE, exposure to white LED triggered very rare but present albumin leakages at doses over 0.09 J/cm$^2$ BLH, along with the presence of a strong albumin staining in the entire photoreceptor segment layer (Fig. 4E, arrow). However, as observed for blue light, accumulation of albumin in the RPE was observed at lower doses. The

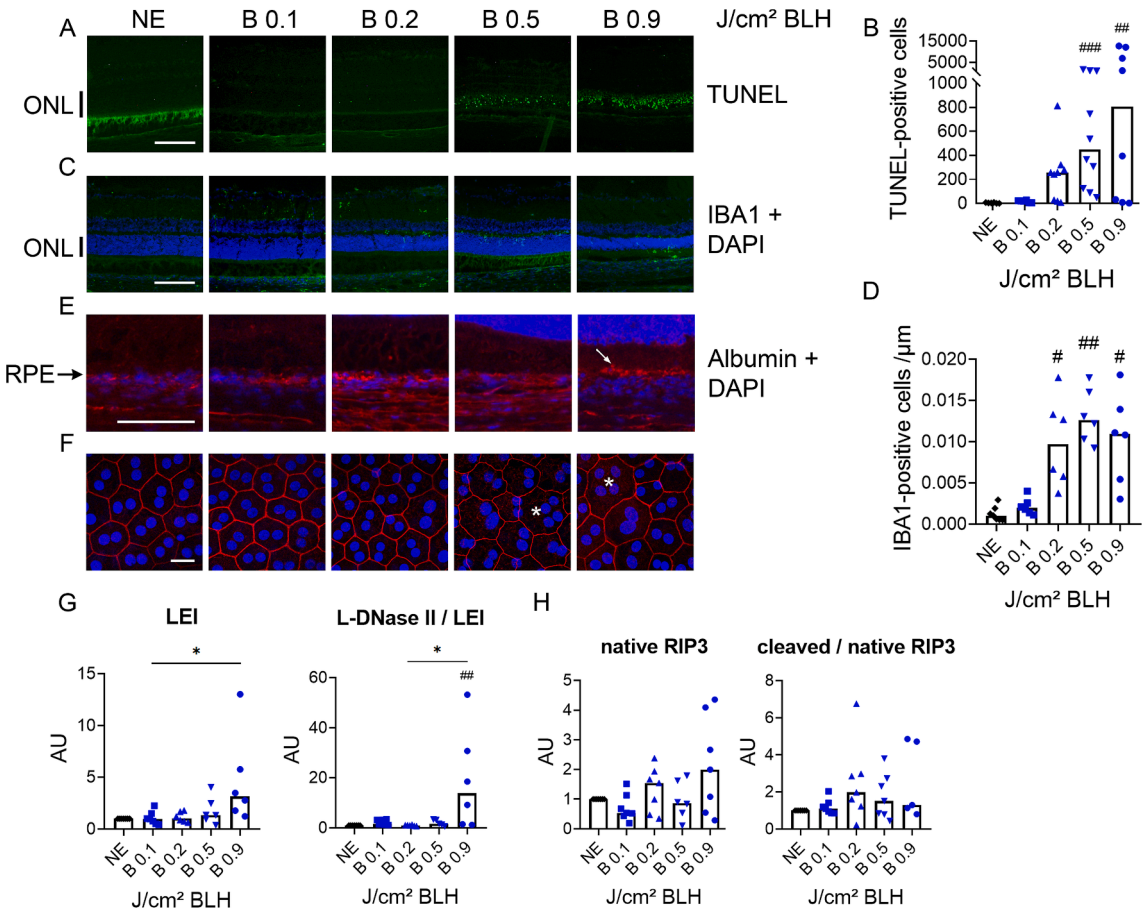


**Fig. 2. Toxicity of blue light at retinal doses under the currently accepted threshold.** A. TUNEL staining on retina sections of rats exposed to increasing BLH-weighted retinal doses of blue (B) LED or non-exposed (NE). ONL: Outer Nuclear Layer. Scale bar = 100 µm. B. Quantification of the TUNEL-positive cell nuclei per eye slice in the ONL of blue LED-exposed retina. H(5) = 20.87, n ≥ 6 eyes. C. Anti-IBA1 (green) and DAPI staining on retina sections of rats exposed to blue LED or non-exposed. ONL: Outer Nuclear Layer. Scale bar = 100 µm. D. Quantification of macrophages invading the neural retina (INL and ONL) of blue LED-exposed rats per analyzed ONL length in µm using IBA1 staining of retinal sections. H(5) = 22.12, n ≥ 6 eyes. E. Anti-albumin immunolabeling (red) and DAPI (blue) on retina sections of rats exposed to blue LED or non-exposed. The arrow shows albumin leakage. RPE: Retinal Pigmented Epithelium. Scale bar = 50 µm. F. Phalloidin (red) and DAPI (blue) staining of RPE flat mounts from rats exposed to increasing doses of light from blue LED. Asterisks correspond to giant polynucleated cells. Scale bar = 20 µm. G,H. Quantification by western blot of the expression of proteins involved in different cell death mechanisms. G. LEI: H(5) = 11.02, n ≥ 6 eyes. L-DNaseII/LEI: H(5) = 18.05, n ≥ 5 eyes. H. RIP3: H(5) = 5.777, n ≥ 6 eyes. Cleaved/native RIP3: H(5) = 5.420, n ≥ 5 eyes. Graphs represent the median. Statistical analysis was made by using the Kruskal-Wallis test followed by Dunn's post-tests. #: significance of the difference compared to NE, #p < 0.05, ##p < 0.01, ###p < 0.001, *: significance of the difference between columns, *p < 0.05, **p < 0.01, ***p < 0.001. Cell death was significantly increased at 0.5 J/cm$^2$ of blue light and over, while IBA1 cells were significantly increased at 0.2 J/cm$^2$. The activated mechanism of cell death was caspase-independent (LEI/L-DNase II). At retinal doses of blue light as low as 0.2 J/cm$^2$ the RPE was challenged, cumulating serum albumin. Leakage of the OBRB appeared at 0.9 J/cm$^2$. Changes in RPE cells morphology (giant cells) were also seen. (For interpretation of the references to colour in this figure legend, the reader is referred to the web version of this article.)

overall structure of the RPE and notably the actin cytoskeleton were also affected (Fig. 4F). Giant multinucleated cells appeared at 0.05 J/cm$^2$ BLH. Sparse openings of the actin barrier were seen at 0.09 J/cm$^2$ BLH and over. Western blot analysis showed no change in the LEI expression, but an increase of L-DNase II at retinal doses of 0.05 J/cm$^2$ BLH and 0.2 J/cm$^2$ BLH suggesting the activation of this caspase-independent apoptotic pathway (Fig. 4G). No activation of the necrosis pathway was identified (Fig. 4H).

### 3.3. Relevance of the BLH weighting

Results displayed on Figs. 2 to 4 highlighted differences in the phototoxicity thresholds for blue and white LED lights when using BLH-weighted retinal doses. In order to better characterize the difference in the retinal reactivity when exposed to the same BLH dose from two different spectra, we used a BLH-weighted dose of 0.2 J/cm$^2$ for blue and white LED. The obtained results are presented in Fig. 5. The number of TUNEL-positive cells in the retina was about 10 times higher after exposure to white LED than after exposure to blue LED, suggesting a higher phototoxicity of white LED (median number of TUNEL-positive cells = 258 and 4660 for blue and white light respectively) (Fig. 5A). Flat mounts of RPE showed an accumulation of rhodopsin aggregates which was greater after exposure to white LED (0.39 % of the total area for non-exposed retinas, 0.45 % for blue light, and 0.84 % for white light) (Fig. 5B, C), suggesting an overload of the clearance of the photoreceptor tips by the RPE. We also recorded a decreased proportion of smaller RPE cells mirrored by an increased proportion of bigger cells after an exposure to white LED exclusively (Fig. 5D). Flat mounts of RPE from rats exposed to white LED displayed a greater proportion of cells containing four or more nuclei (0.00 % for non-exposed retinas, 0.33 % for blue light, and 0.72 % for white light) (Fig. 5E).

### 3.4. Retinal stress response after exposure to light

Retinal stress response was analyzed in the Müller cells by an anti-glial fibrillary acid protein (GFAP) staining of retina sections

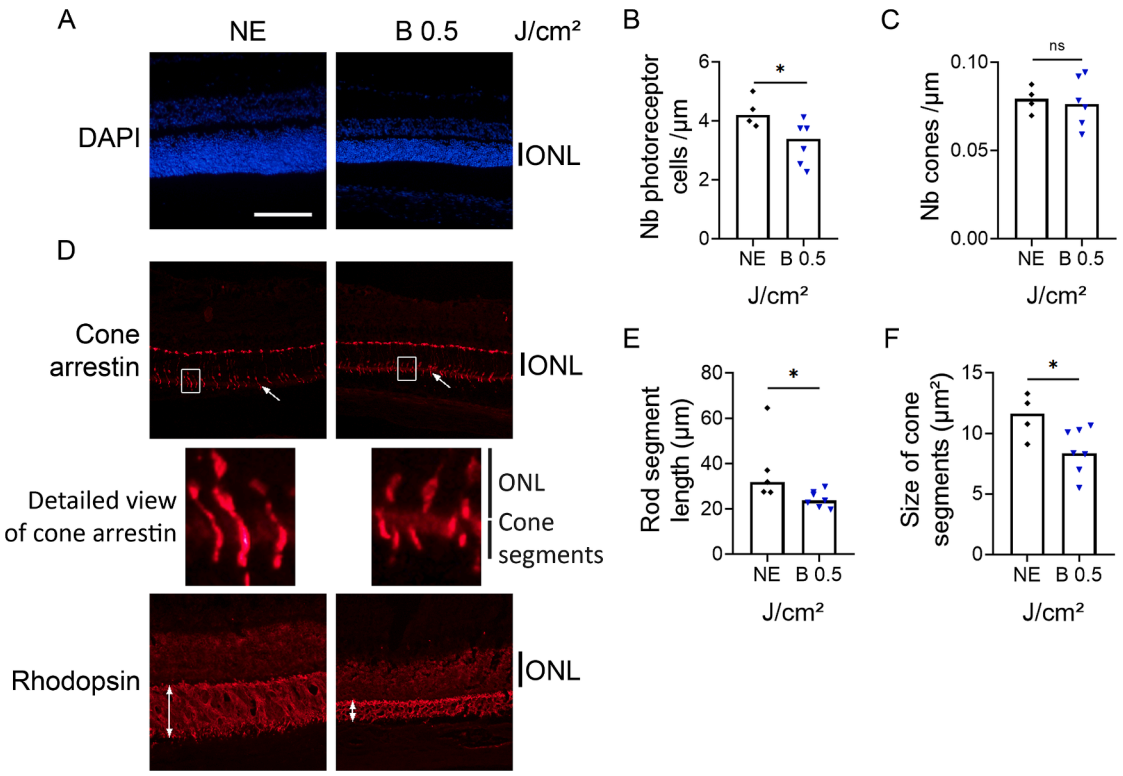


**Fig. 3. Light-induced damagein rat retina 1 week after exposure to blue LED at the BLH-weighted retinal dose of 0.5 J/cm².** A. Overall retinal structure with DAPI staining on retina sections of rats exposed to blue (B) LED or non-exposed (NE). ONL: Outer Nuclear Layer. Scale bar = 100 µm. B. Quantification of the number of photoreceptors per analyzed ONL length in µm in the superior part of the retina section of each eye using the DAPI staining of the ONL. U = 9, n ≥ 4 eyes. C. Counting of the number of cones per analyzed ONL length in µm in the superior part of the retina section of each eye using the cone arrestin staining. U = 11, n ≥ 4 eyes. D. Light damage on photoreceptors. Upper row: anti-cone arrestin staining on retina sections. Arrows show cone segments. White rectangles corresponds to the detailed views shown below. Lower row: anti-rhodopsin staining on retina sections. Double head arrows highlight the thickness of the rod segment layer. ONL: Outer Nuclear Layer. Scale bar represents 100 µm. E. Measurement of the length of the rod segment layer in the superior part of the retina section of each eye using the rhodopsin staining. U = 3, n ≥ 4 eyes. F. Quantification of the size of cone segments in the superior part of the retina section of each eye using the cone arrestin staining. U = 3, n ≥ 4 eyes. Graphs represent the median. Statistical analysis was performed using the Mann-Whitney test. ns: non-significant, *p < 0.05. A decrease in the ONL thickness was seen with a significant decrease in the total photoreceptors number. Cones are less affected but a decreased length of both cones and rods photoreceptors outer segments was seen. (For interpretation of the references to colour in this figure legend, the reader is referred to the web version of this article.)

(Fig. 6A). An increase of GFAP was already visible at 0.1 J/cm$^2$ for blue LED and 0.01 J/cm$^2$ BLH for white LED. Other proteins involved in stress responses were analyzed by western blot. We found a decrease in heat shock protein 70 (HSP70), statistically significant for blue light exposure from 0.1 J/cm$^2$ (Fig. 6B) and white light exposure from 0.02 J/cm$^2$ BLH (Fig. 6C). No increase in the expression of p62 (also called sequestosome 1, involved in autophagy and other processes) was observed. However, the amount of p62 aggregates increased for the highest tested doses, which correspond to 0.9 J/cm$^2$ for blue LED (Fig. 6D) and 0.2 J/cm$^2$ BLH for white LED (Fig. 6E).

### 3.5. *Importance of the spectral composition on phototoxicity*

The differences in the phototoxicity of blue and white LED suggested an impact of parts of the spectrum of the white LED other than the blue component. In order to investigate this point, we distributed the energy of the white light between a blue light and a green light, which are the components involved in phototoxicity. Thus, the red component is excluded as it is hypothesized not to be involved in phototoxicity. To get closer to the spectral distribution of the white LED, we exposed our rats to blue LED at a total retinal dose of 0.1 J/cm$^2$, to green LED at 0.8 J/cm$^2$, or to white LED at 0.9 J/cm$^2$ (the integrated spectrum of each light was used to calculate the energy received by the retina).

TUNEL staining and anti-IBA1 staining were considered on retinal sections (Fig. 7A). Photoreceptor's death, as shown by TUNEL labeling, was statistically significant after exposure to the green and white LED (TUNEL-positive cells: 4.00 for non-exposed retinas, 20.50 for blue light, 1481 for green light, and 2621 for white light) (Fig. 7B). The number of microglial cells invading the retina was also significantly enhanced after exposure to green and white lights (0.001 cells/µm for NE, 0.002 for B, 0.016 for G, and 0.011 for W) (Fig. 7C). Anti-LEI/L-DNase II staining on the most damaged area of the retina, however, showed the activation of LEI/L-DNase II pathway (nuclear staining of photoreceptors) mostly after exposure to blue and white LED (Fig. 7D). Quantification of the expression of LEI/L-DNase II and RIP3 by western blot of total retina samples showed no changes when animals were exposed to green LED (Fig. 7E, 7F). L-DNase II was however significantly increased by the exposure to blue LED (Fig. 7E).

The stress response analysis showed a stronger GFAP staining mostly after exposure to white LED at 0.9 J/cm$^2$, but not after exposure to blue or green LED (Fig. 8A). This was confirmed by western blot quantification (Fig. 8B).

Concerning HSP70, exposure to blue LED at 0.1 J/cm$^2$ induced a significant reduction of its expression as compared to non-exposed retinas or to retinas exposed to white light at 0.9 J/cm$^2$ (Fig. 8C). The quantity of p62 protein or p62 aggregates remained unchanged for blue, green and white LED at the given doses (Fig. 8D, 8E).

Other than their important emission in the blue part of the spectrum, white LED also displayed a weak emission in the red part of the visible spectrum if compared to older lighting devices. We studied the impact of the addition of a red component to white LED by exposing the rats to white LED at 0.9 J/cm$^2$ or red LED at 0.1 J/cm$^2$ alone, or white and red

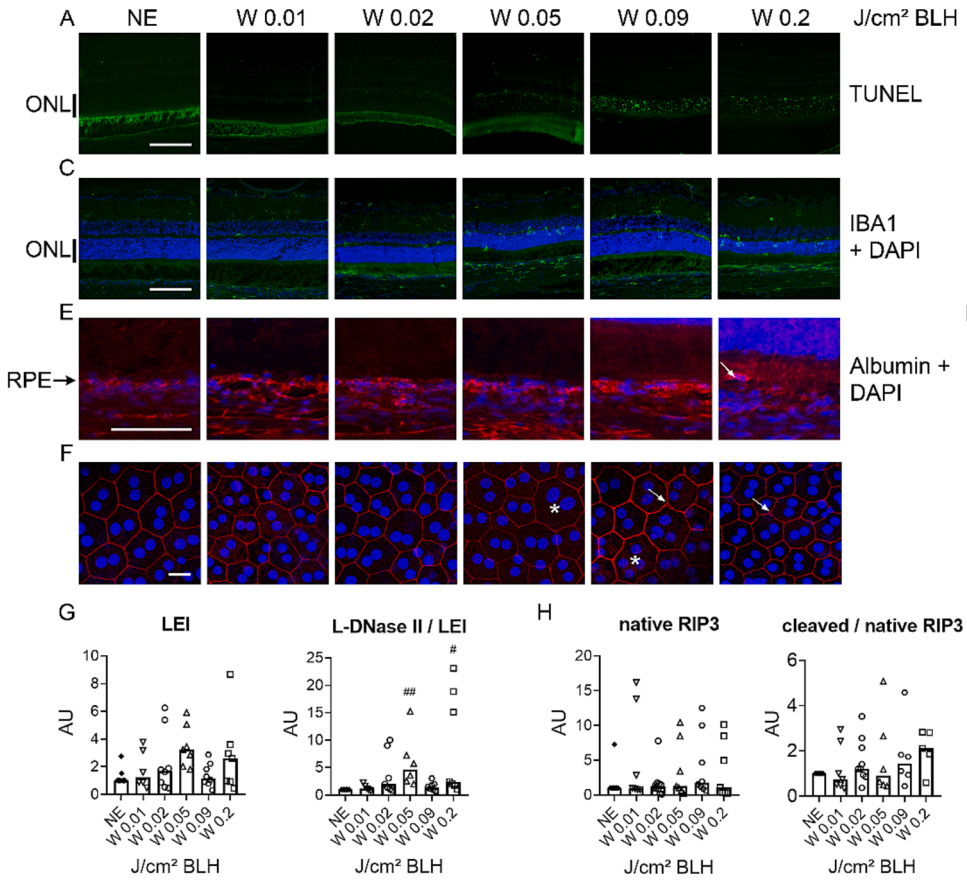


**Fig. 4. Toxicity of a polychromatic light at retinal doses under the accepted threshold.** A. TUNEL staining on retina sections of rats exposed to increasing BLH-weighted retinal doses of white (W) LED or non-exposed (NE). ONL: Outer Nuclear Layer. Scale bar = 100 µm. B. Quantification of the TUNEL-positive cell nuclei per eye slice in the ONL of white LED-exposed retina at different doses. $H(6) = 27.61$, $n \geq 6$ eyes. C. Anti-IBA1 (green) and DAPI staining on retina sections of rats exposed to white LED at different doses or non-exposed. ONL: Outer Nuclear Layer. Scale bar = 100 µm. D. Quantification of macrophages invading the neural retina (INL and ONL) of white LED-exposed rats per analyzed ONL length in µm using IBA1 staining of retinal sections. $H(6) = 25.44$, $n \geq 6$ eyes. E. Anti-albumin (red) and DAPI immunolabeling on retina sections of rats exposed to white LED at different doses or non-exposed. The arrow shows albumin leakage. RPE: Retinal Pigmented Epithelium. Scale bar = 50 µm. F. Phalloidin (red) and DAPI (blue) staining of RPE flat mounts from rats exposed to increasing doses of white LED. Asterisks correspond to giant polynucleated cells. Arrows show alterations of the actin barrier. Scale bar = 20 µm. G,H. Quantification by western blot of the expression of proteins involved in different cell death mechanisms. G. LEI: $H(6) = 8.629$, $n \geq 6$ eyes. L-DNaseII/LEI: $H(6) = 19.11$, $n \geq 5$ eyes. H. RIP3: $H(6) = 2.054$, $n \geq 7$ eyes. Cleaved/native RIP3: $H(6) = 3.881$, $n \geq 5$ eyes. Graphs represent the median. Statistical analysis was made by using the Kruskal-Wallis test followed by Dunn's post-tests. #: significance of the difference compared to NE, #$p < 0.05$, ##$p < 0.01$, ###$p < 0.001$, *: significance of the difference between columns, *$p < 0.05$. When exposed to a white BLH-weighted light, cell death and retinal infiltration by IBA-1 cells were seen after exposure to 0.09 J/cm$^2$ and 0.05 J/cm$^2$ respectively. At retinal BLH-weighted doses of white light of 0.05 J/cm$^2$ the RPE was challenged cumulating serum albumin. Leakage of the OBRB appeared at 0.09 J/cm$^2$. Changes in RPE cells morphology (giant cells) were also seen (asterisks) and openings of the RPE layer was found (arrows). Caspase-independent activated cell death was seen after exposure to 0.05 J/cm$^2$ BLH-weighted of white light. (For interpretation of the references to colour in this figure legend, the reader is referred to the web version of this article.)

LED simultaneously corresponding to a total retinal dose of 1.0 J/cm$^2$ (Fig. 9).

Exposure of rats to white LED alone triggered cell death in the retina (Fig. 9A, B), as revealed by TUNEL staining, while exposure to red LED did not. Interestingly, addition of the red light to white LED visibly reduced the number of apoptotic cells compared to an exposure to white LED alone, as observed with the TUNEL staining, although this decrease appeared non-significant (TUNEL-positive cells: 4.00 for non-exposed retinas, 2621 for white light, 854 for white plus red light, and 7.00 for red light). In contrast, the inflammatory response, evaluated by the infiltration of microglia in the retina, did not decrease when red LED was added to the white LED (IBA1-positive cells /µm: 0.001 for non-exposed retinas, 0.011 for white light, 0.010 for white plus red light, and 0.001 for red light) (Fig. 9C) suggesting that red light mostly has an impact on cell death but not on the inflammatory response. The activation and nuclear translocation of L-DNase II in photoreceptor's nuclei was visible on the most damaged part of retina after exposure to white LED alone (Fig. 9D) but it was reduced by the addition of red light (Fig. 9D). Quantification by western blot showed that the addition of red to the white light, or red light alone did not significantly change the amount of LEI, L-DNase II (Fig. 9E), RIP3 or cleaved RIP3 (Fig. 9F), indicating that the activation of cell death was limited to the most exposed part of the retina.

The GFAP staining was also slightly increased after exposure to white LED alone or white and red LED simultaneously compared to non-exposed retinas or retinas only exposed to red LED (Fig. 10A). Quantification by western blot of GFAP supported this result (Fig. 10B). No change in the HSP70 expression was found after exposure to the different conditions (Fig. 10C). However, the amount of p62 protein was significantly increased after exposure to white plus red LED, but not after exposure to red or white light alone (Fig. 10D). The quantity of p62 aggregates did not significantly change in any condition (Fig. 10E).

## 4. Discussion

In current regulations (EU 62471), limit exposure values (LEV) to

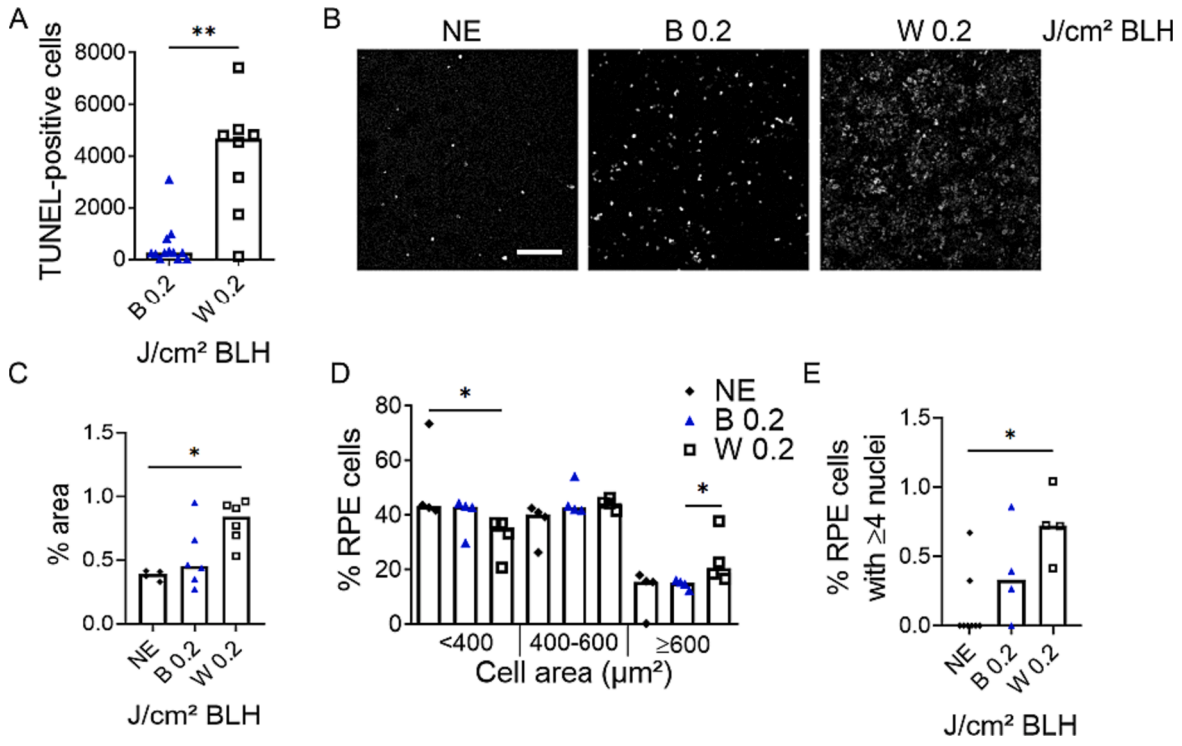


**Fig. 5. Comparison of light-induced damagein rat retina after exposure to blue and white LED at the same BLH-weighted retinal dose of 0.2 J/cm².** A. Quantification of TUNEL-positive cells per eye slice in the ONL from rats exposed to blue (B) or white (W) LED at 0.2 J/cm² BLH-weighted. Statistical significance was evaluated using the Mann-Whitney test. U = 10, n ≥ 8 eyes. **p < 0.005. B. Anti-rhodopsin staining in RPE flat-mount from rats exposed to blue (B) or white (W) LED at 0.2 J/cm² BLH-weighted or non-exposed (NE). Scale bar = 20 µm. C. Ratio of the RPE flat-mount surface covered by rhodopsin aggregates. Statistical analysis was evaluated using the Kruskal-Wallis test followed by Dunn's post-tests. H(3) = 7.783, n ≥ 4 eyes. *p < 0.05. D. Distribution of the RPE cell area from rats exposed to blue (B) or white (W) LED at 0.2 J/cm² BLH-weighted or non-exposed (NE). Statistical analysis was evaluated using the Kruskal-Wallis test followed by Dunn's post-tests. < 400 µm2: H(3) = 5.115; 400–600 µm2: H(3) = 4.962; ≥600 µm2: H(3) = 6.577,*p < 0.1, n ≥ 4 eyes. Cell area was obtained using phalloidin staining on RPE flat mounts. E. Ratio of RPE cells that possess 4 or more nuclei in RPE flat-mount from rats exposed to blue (B) or white (W) LED at 0.2 J/cm² BLH-weighted or non-exposed (NE). Statistical analysis was evaluated using the Kruskal-Wallis test followed by Dunn's post-tests. H(3) = 8.095, n ≥ 4 eyes. *p < 0.05. Graphs represent the median. When compared at the same BLH-weighted dose, white light is more damaging than blue light. (For interpretation of the references to colour in this figure legend, the reader is referred to the web version of this article.)

visible light are designed to protect the human retina from damage induced by artificial sources. Although these regulations concern humans, the basic restrictions rely on data obtained from monkeys and the spectrum action curves designed for this animal (van Norren and Gorgels, 2011). Interestingly, the paper of Van Norren and Gorgels shows the same curves for rodents (rats, mice, squirrels, albino or pigmented), obtained by the same analytical methods, showing that the rodent retina is twice as sensitive as the primate retina, with a sensitivity threshold for blue light of 11 J/cm² for rodents compared to 22 J/cm² for primates.

### 4.1. *The use of the retinal dose and albino rats*

As stated in the paragraph above, the light exposure used in the normative is the retinal dose. This represents the amount of energy that reaches the retina. It depends on the irradiance of the light source and on the time of exposure. Actually, Ham et al showed in their seminar paper (Ham et al., 1982) that after an exposure of aphakic monkeys to a 325 nm light, either during 100 s at a retinal irradiance of 50 mW/cm² or 1000 s at 5 mW/cm², the retinal damage was equivalent, showing that the most important factor is the final retinal dose of 5 J/cm². When considering retinal damage, retinal illuminance rather than the room or corneal illuminance should be evaluated. This depends on the animal model and the light exposure protocol. Hence, for *in vivo* models, the geometry of the animal eye and face, the absorbance of the ocular media and tissues located in front of the retina, the position of the light source, along with the movements of the animal affect the proportion of light that will reach the retina. For this reason, and in order to give more precise information, we use the retinal dose in this paper.

Finally, the use of the retinal dose also corrects another important exposure parameter related to retinal exposure to light: the focal distance. As shown in Materials and Methods (section 2.4.), the retinal exposure is inversely proportional to 8 fold the square of the focal distance. So a rat (focal distance of 5 mm) exposed to the same environmental light during the same exposure time as a human (focal distance of 22 mm) will have a retinal exposure 20 fold higher just because of this parameter. This explains why the rat (and in fact most of the rodents) seem extremely sensitive to light while, in fact, if the actual exposure of the retina is taken into account, rodents are only twice as sensitive as primates (van Norren and Gorgels, 2011).

According to this, the retinal dose can be changed by changing the irradiance or by changing the time of exposure. In our experimental setting we decided to change the time of exposure for the following reasons: first it was the easiest way of obtaining precise doses with minimal changes. Second, as this study aims at simulating artificial domestic lighting, the exposure of the retina changes in the same room mostly by changing the time of exposure rather than changing the intensity of light. It could be argued that light intensity can be easily modulated with a variator. However, as we use LED technology in this work, light intensity is usually regulated by using the PWM (Pulse width modulation) technology. This induces a flickering over 100 Hz not seen by most humans. However, as the effect of flickering on phototoxicity is not known, we do not want to introduce this additional variable in our study. We also want to stress that the use of photometric measurements

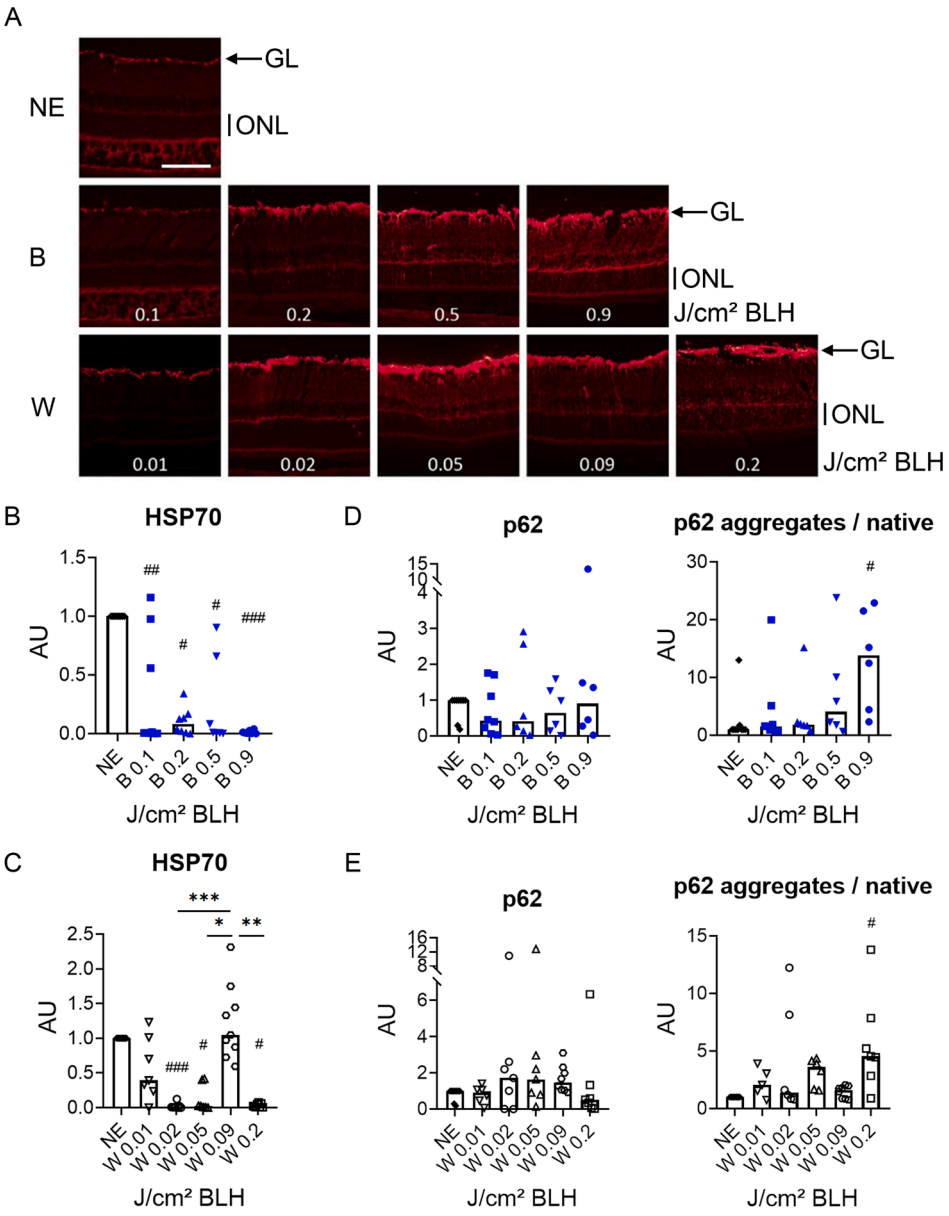


**Fig. 6. Cellular stress in neural retina after exposure to blue and white LED.** A. Anti-GFAP immunolabeling on retina sections from rats exposed to blue (B) or white (W) LED at increasing BLH-weighted retinal doses or non-exposed rats (NE). GL: Ganglion Layer, ONL: Outer Nuclear Layer, scale bar = 100 μm. B-E. Quantification in the retina of proteins involved in stress response by western blot. B. $H(5) = 19.65$, $n \geq 7$ eyes. C. p62: $H(5) = 0.8319$, $n \geq 6$ eyes. p62 aggregates/native: $H(5) = 11.62$, $n \geq 6$ eyes. D. $H(6) = 32.89$, $n \geq 7$ eyes. E. p62: $H(6) = 8.333$, $n \geq 6$ eyes. p62 aggregates/native: $H(6) = 13.48$, $n \geq 5$ eyes. Graphs represent the median. Statistical analysis was done by using the Kruskal-Wallis test followed by Dunn's post-tests. #: significance of the difference compared to NE, #$p < 0.05$, ##$p < 0.01$, ###$p < 0.001$, *: significance of the difference between columns, *$p < 0.05$, **$p < 0.01$, ***$p < 0.001$. GFAP-positive Müller cells were seen at 0.5 J/cm$^2$ of BLH-weighted blue light and 0.05 J/cm$^2$ BLH-weighted white light. HSP70 is decreased under blue light alone and p62 aggregates increased at the highest doses of light. (For interpretation of the references to colour in this figure legend, the reader is referred to the web version of this article.)

(in lux) in this kind of work is not applicable and should be seriously avoided. Illuminance is not a direct measurement but a weighting of the spectrum according to the human eye sensitivity, that is the V(λ) (luminous efficiency function), it aimed to be used for polychromatic light and not for monochromatic light (coherent or incoherent). Please note that its use even for polychromatic light induces the loss of information of the blue and red part of the spectrum.

It is currently believed that the retina of albino animals is intrinsically more sensitive to light than the retina of pigmented animals. This assumption is right if we consider animals exposed to the same environmental light for the same exposure time. However, if we consider the amount of light that reaches the retina, it is clear that this « obvious » statement is a mistake. The retina of an albino and a pigmented animal is not exposed the same way under the same light. It is not receiving the same retinal dose. As seen in Material and Methods (section 2.4.), the retinal illuminance is proportional to the square of the pupilar diameter. Here lays the big difference between pigmented and non-pigmented animals, as in albino animals the iris is very inefficient in decreasing the retinal illuminance. This is why in the action spectrum curves of Van Norren, done by using the retinal doses (van Norren and Gorgels, 2011), it can be seen that albino and pigmented rats have the same sensitivity to light (see also Gorgels and van Norren, 1995 and 1998, where the retinal sensitivity of Long Evans (pigmented) and Wistar (albino) rats is compared (Gorgels and Van Norren, 1998; Gorgels and van Norren, 1995)).

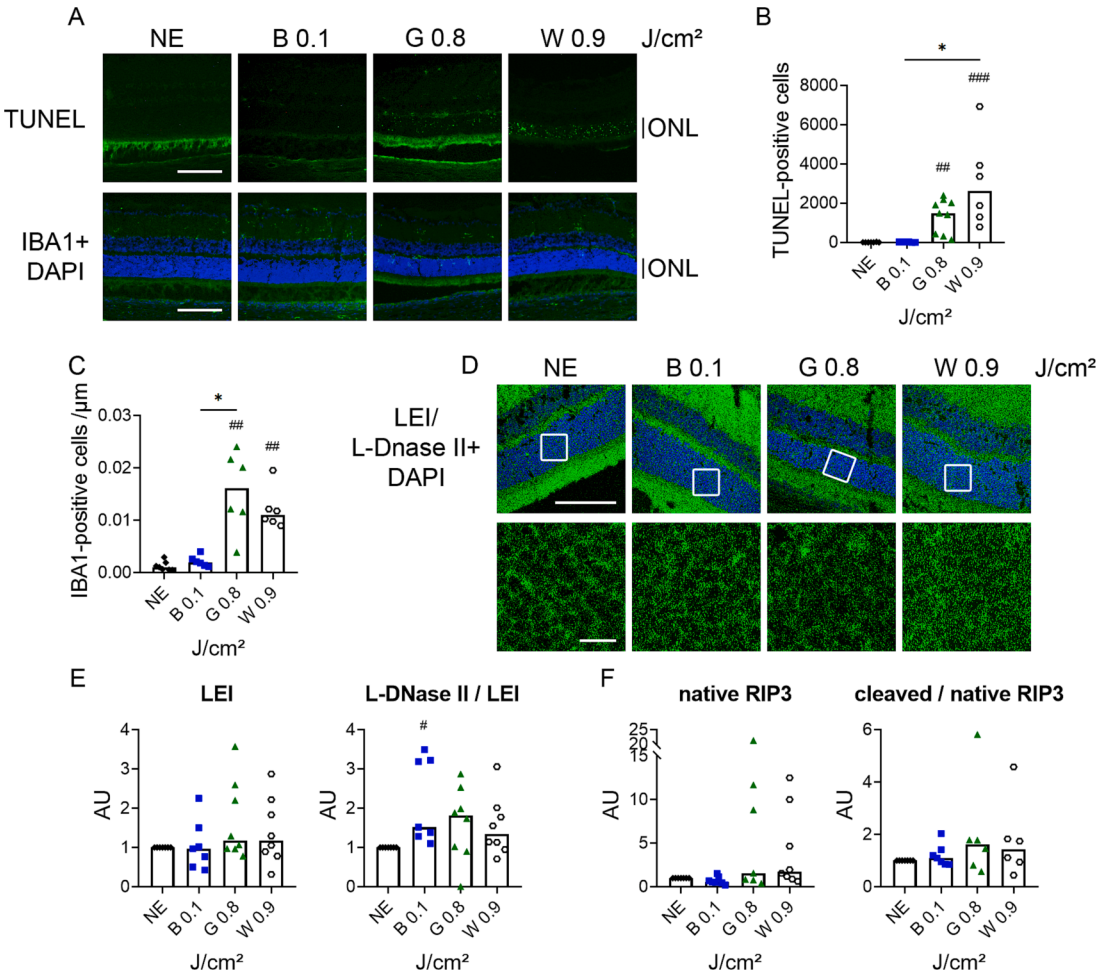


**Fig. 7. Effect of the different spectral components in white LED phototoxicity on the neural retina.** A. Upper row: TUNEL staining (green), lower row: anti-IBA1 (green) and dapi (blue) labeling, on retina sections of rats exposed to green (G), blue (B), or white (W) LED or non-exposed (NE). Used retinal doses were calculated to represent the decomposition of the white LED into blue + green LED. ONL: Outer Nuclear Layer, scale bar = 100 µm. B. Quantification of TUNEL-positive cell nuclei per eye slice in the ONL. $H(4) = 21.23$, $n \geq 6$ eyes. C. Quantification of macrophages invading the neural retina (INL and ONL) per analyzed ONL length in µm of rats exposed to green (G), blue (B), or white (W) LED or non-exposed (NE) using anti-IBA1 staining of retinal sections. $H(4) = 18.79$, $n \geq 6$ eyes. D. Anti-LEI/L-DNase II + DAPI immunostaining on retina sections of rats exposed to green (G), blue (B), or white (W) LED or non-exposed (NE). ONL: Outer Nuclear Layer, scale bar = 100 µm. Lower panel shows a zoom in the ONL layer of the retina sections. Scale bar = 10 µm. E, F. Quantification by western blot of proteins involved in caspase-independent apoptosis and necroptosis in the retina of rats exposed to green (G), blue (B), or white (W) LED or non-exposed (NE). E. LEI: $H(4) = 2.178$, $n \geq 7$ eyes. L-DNase II/LEI: $H(4) = 8.627$, $n \geq 7$ eyes. F. RIP3: $H(4) = 7.482$, $n \geq 7$ eyes. Cleaved/native RIP3: $H(4) = 1.522$, $n \geq 6$ eyes. Graphs represent the median. Statistical analysis was evaluated using the Kruskal-Wallis test followed by Dunn's post-tests. #: significance of the difference compared to NE, #$p < 0.05$, ##$p < 0.01$, ###$p < 0.001$, *: significance of the difference between columns, *$p < 0.05$. The effect of blue and green wavelength of white light were separately tested for cell death and inflammation, showing that the blue component is mostly responsible for the activation of caspase-independent cell death and the green component for the inflammatory reaction. (For interpretation of the references to colour in this figure legend, the reader is referred to the web version of this article.)

### *4.2. Phototoxicity and light spectrum*

Current phototoxicity thresholds for a light source are based on the blue part of the spectrum, and rely on a weighting of the spectrum by the B(λ) curve, the blue light hazard (BLH) weighting (International Commission on Non-Ionizing Radiation Protection, 2013). Therefore, BLH-weighted doses are used in this study. Interestingly, we use an animal model with a "realistic exposure" as the animal is free to move. Our results indicate that when rats are exposed to blue light alone (Figs. 2 and 3, parts of Figs. 5, 6, 7 and 8), the phototoxicity threshold for rats would be around 0.2 J/cm$^2$. This value is 50 fold lower than the value that can be calculated from van Norren and Gorgels (11 J/cm$^2$) (van Norren and Gorgels, 2011). This difference probably relies on the difference of methods for evaluating the loss of photoreceptors. We use here the very sensitive TUNEL assay and not direct ophthalmoscopy or global electroretinogram which are less sensitive. Moreover, in the analysis of cell death, we use a modified TUNEL assay (Lebon et al., 2015) allowing the detection of caspase-independent cell death, very frequently seen in the retina (Françon and Torriglia, 2023; Torriglia et al., 2016). Compared to classical TUNEL assay, a 3-fold increase in the number of labeled cells is seen (Supplementary Fig. 2). Interestingly, this is a significant result because it leads to a definitive loss of photoreceptors as seen 1 week after exposure (Fig. 3) so that, the TUNEL-positive cells observed right after light exposure truly result in a significant loss of photoreceptors.

In this study we used a blue light peaking at 449 nm because this is the peak of the BLH weighting. Other authors and ourselves used different spectra of blue light, peaking from 405 to 473 nm (Feng et al., 2021; Heinig et al., 2020; Hu et al., 2016; Jaadane et al., 2015; Tang et al., 2021; Zhuang et al., 2021). In each case retinal degeneration was induced but the mechanism of cell death involved was not always the same. This seems to depend mostly on the dose received by the retina, which is very different between studies (from 0.5 to 53 J/cm$^2$).

When studying commercially available white LED (Figs. 4, 5, 6)

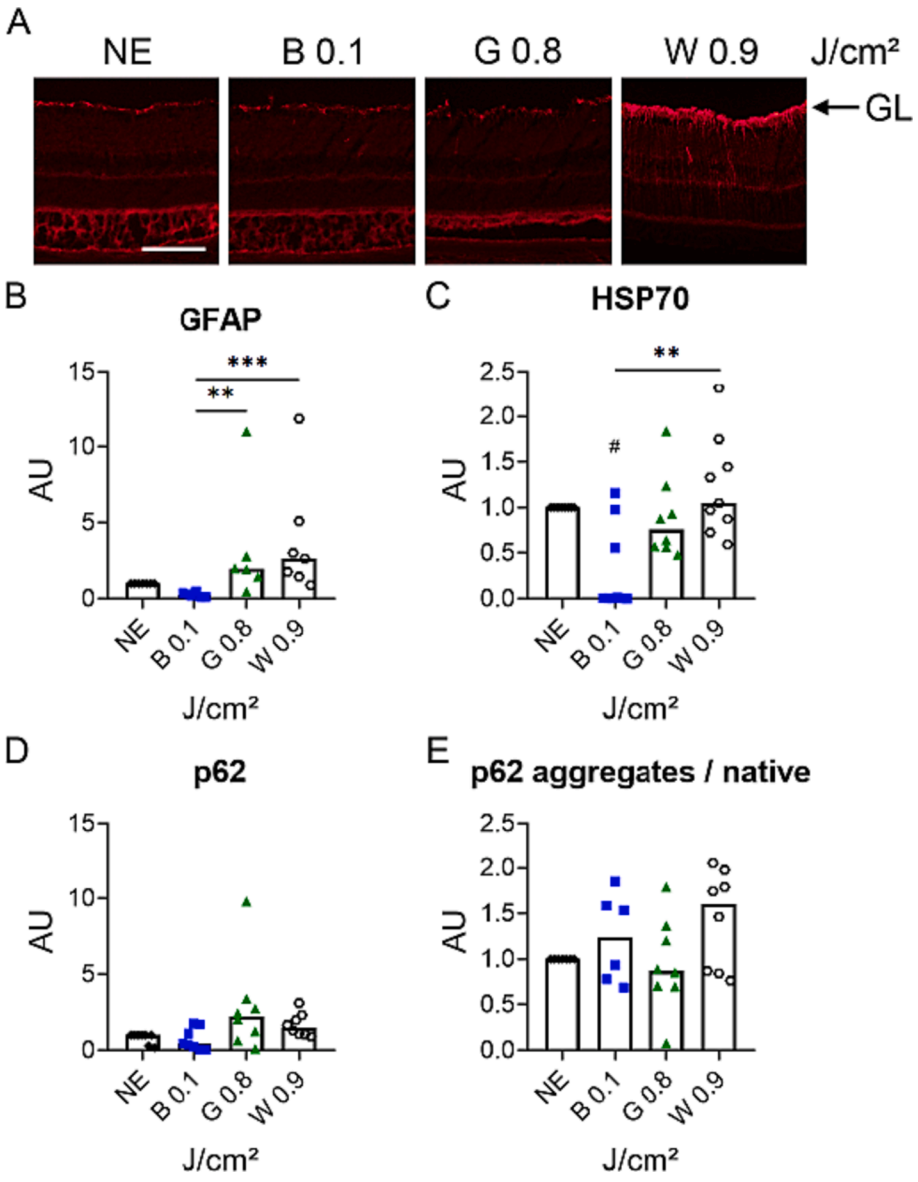


**Fig. 8. Effect of the different spectral components in the cellular stress response of the retina.** A. Anti-GFAP immunolabeling on retina sections from rats exposed to blue (B), green (G), white (W) LED or non-exposed (NE). GL: Ganglion Layer. Scale bar = 100 µm. B-E. Quantification by western blot of proteins involved in the stress response of the retina of rats exposed to blue (B), green (G), white (W) LED or non-exposed (NE). B. $H(4) = 17.00$, $n \geq 6$ eyes. C. $H(4) = 13.20$, $n \geq 8$ eyes. D. $H(4) = 10.42$, $n \geq 8$ eyes. E. $H(4) = 3.046$, $n \geq 6$ eyes. Graphs represent the median. Statistical analysis was evaluated using the Kruskal-Wallis test followed by Dunn's post-tests. *: significance of the difference between columns, **$p < 0.01$, ***$p < 0.001$. Green light was involved in the Müller cells stress response (GFAP) while blue light generated à decrease in the expression of HSP70. (For interpretation of the references to colour in this figure legend, the reader is referred to the web version of this article.)

using BLH-weighted doses, the phototoxicity threshold is overestimated by a factor of 550 (Fig. 4). If the total retinal dose is considered (not the BLH-weighted dose), the threshold for white LED is 0.2 J/cm$^2$, the same as for blue light, suggesting that the blue component is not solely having an impact on phototoxicity. Note that the blue component of this light represents about 10 % of the total spectrum (in our experimental setting). Interestingly, our results also suggest an enhanced effect of blue and green light, as phototoxicity of white light is higher than the one generated by the addition of blue or green light considered separately. Although additional experiments combining green and blue LED simultaneously should be performed to verify this point, these results taken together indicate that the spectral composition of a polychromatic light source, and not only one sector of the spectrum, influences its phototoxicity and raise questions regarding the relevance of BLH weighting to evaluate the phototoxicity of a light source. Note that here we analyze the different wavelengths as represented in the white LED spectrum. In these conditions, the dose for green light is higher than the one for blue light, and we observe a higher impact of the green light on the phototoxicity of white light. It has been argued that the rapid bleaching of rhodopsin induced by green light could contribute to retinal protection in cone-rich areas of the retina, as the macula (Wu et al., 2006). However, in humans, and mostly in children, the accidents with green lasers inducing maculopathies are frequent (Torp-Pedersen et al., 2018) and damage the retina severely and permanently (Mtanes et al., 2018).

Commercially available white LED are also characterized by a small proportion of the red part of the spectrum (Françon and Torriglia, 2023), as compared with halogen or incandescent sources. It was shown that, in the skin and the retina, red light can activate stress pathways, a property that has been used in skin healing studies following UV-induced damage

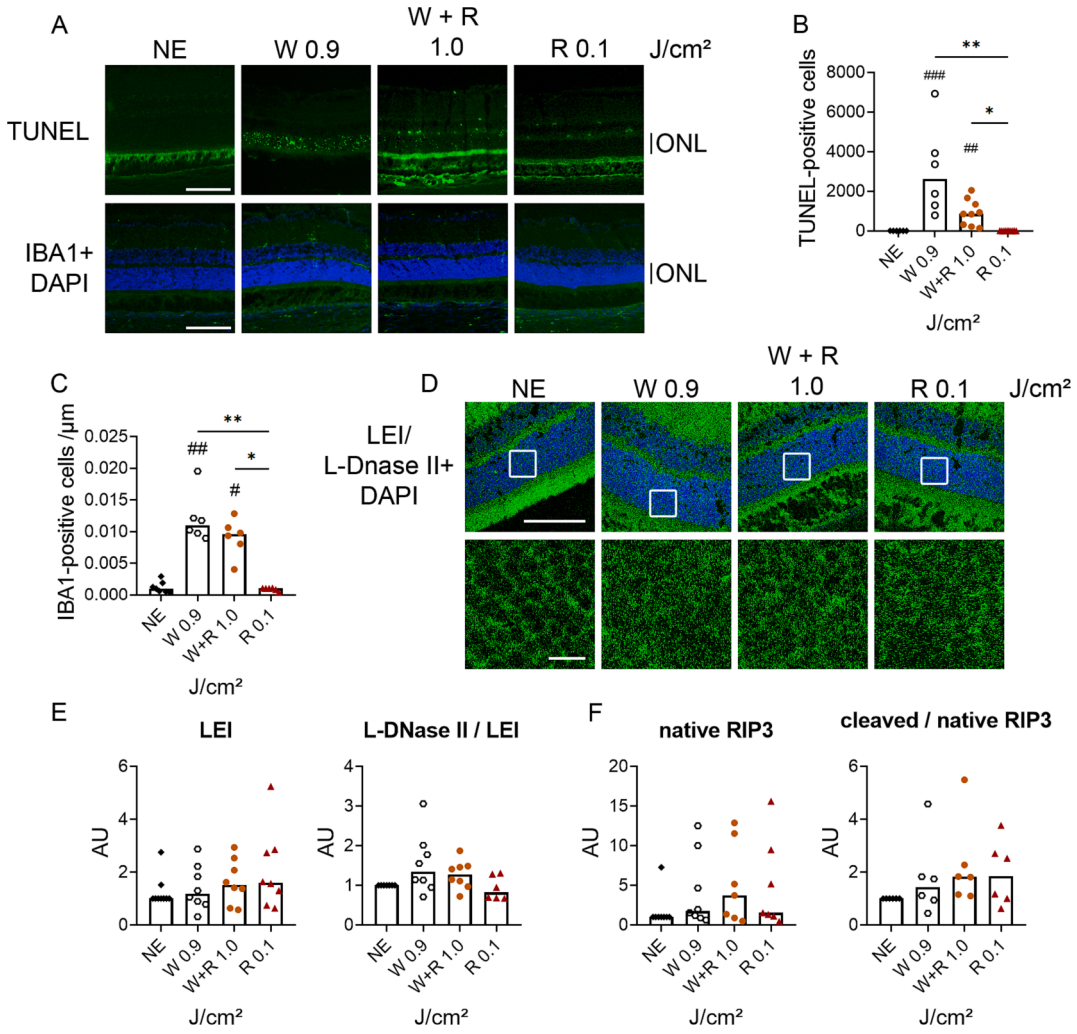


**Fig. 9. Effect of the red component in white LED phototoxicity on the neural retina.** A. Upper row: TUNEL staining (green), lower row: anti-IBA1 (green) and DAPI (blue) labeling, on retina sections of rats exposed to white (W) or red (R) LED only, or to white and red LED simultaneously (W + R) or non-exposed (NE). ONL: Outer Nuclear Layer, scale bar = 100 µm. B. Quantification of TUNEL-positive cell nuclei per eye slice in the ONL. $H(4) = 23.20$, $n \geq 6$ eyes. C. Quantification of macrophages invading the neural retina (INL and ONL) per analyzed ONL length (µm) of rats exposed to white (W) or red (R) LED only, or to white and red LED simultaneously (W + R) or non-exposed (NE) using anti-IBA1 staining of retinal sections. $H(4) = 18.32$, $n \geq 6$ eyes. D. Anti-LEI/L-DNase II + DAPI immunostaining on retina sections of rats exposed to white (W) or red (R) LED only, or to white and red LED simultaneously (W + R) or non-exposed (NE). ONL: Outer Nuclear Layer, scale bar = 100 µm. Lower panel shows a zoom in the ONL layer of the retina sections. Scale bar = 10 µm. E, F. Quantification by western blot of proteins involved in caspase-independent apoptosis and necroptosis in the retina of rats exposed to white (W) or red (R) only, or to white and red LED simultaneously (W + R) or non-exposed (NE). E. LEI: $H(4) = 2.047$, $n \geq 8$ eyes. L-DNase II/LEI: $H(4) = 6.813$, $n \geq 6$ eyes. F. RIP3: $H(4) = 3.140$, $n \geq 7$ eyes. Cleaved/native RIP3: $H(4) = 7.392$, $n \geq 6$ eyes. Graphs represent the median. Statistical analysis was evaluated using the Kruskal-Wallis test followed by Dunn's post-tests. #: significance of the difference compared to NE, #$p < 0.05$, ##$p < 0.01$, ###$p < 0.001$, *: significance of the difference between columns, *$p < 0.05$, **$p < 0.01$, ***$p < 0.001$. The addition of red wavelengths to white light tended to decrease the number of TUNEL-positive cells and the nuclear translocation of L-DNase II. (For interpretation of the references to colour in this figure legend, the reader is referred to the web version of this article.)

(Kim et al., 2017), to protect the RPE from hypoxia-induced damage (Kim and Won, 2022), and to mitigate the retinal damage induced by light (Nie et al., 2022). In accordance with these results, our study shows that the addition of red LED to white LED partially protects against photoreceptor cell death, highlighting the need for considering the whole spectrum in the evaluation of phototoxicity.

### 4.3. Cellular stress and cell death in phototoxicity

In this paper, we also analyze the cell death mechanisms induced by exposure to low doses of light. We only observe the presence of caspase-independent apoptosis and show the importance of the blue component in the activation of this pathway. This differs from the results obtained with higher doses of blue and white light where necrosis is also induced (Jaadane et al., 2015). It also indicates that different doses of light can induce different mechanisms of cell death, clearly showing that the use of a single method to evaluate cell death might lead to an underestimation of this phenomenon.

Other than cell death, light exposure also activates a retinal inflammatory response with the infiltration of microglial and macrophages cells. Results shown in Fig. 7 indicate that the green component has a heavy weight in this response.

Other stress proteins are analyzed. This includes GFAP, involved in glial response, the heat shock protein 70 (HSP70) involved in cell survival (Moradi-Marjaneh et al., 2019) and in DNA damage repair (Choi et al., 2016; Kotoglou et al., 2009), and p62 involved in stress response and autophagy. Extremely low doses of blue and white light are sufficient to trigger the increase of GFAP in the Müller cells. HSP70, which is mainly known to be increased under different stress, surprisingly decreases under blue and white light exposure, a response seen in aging

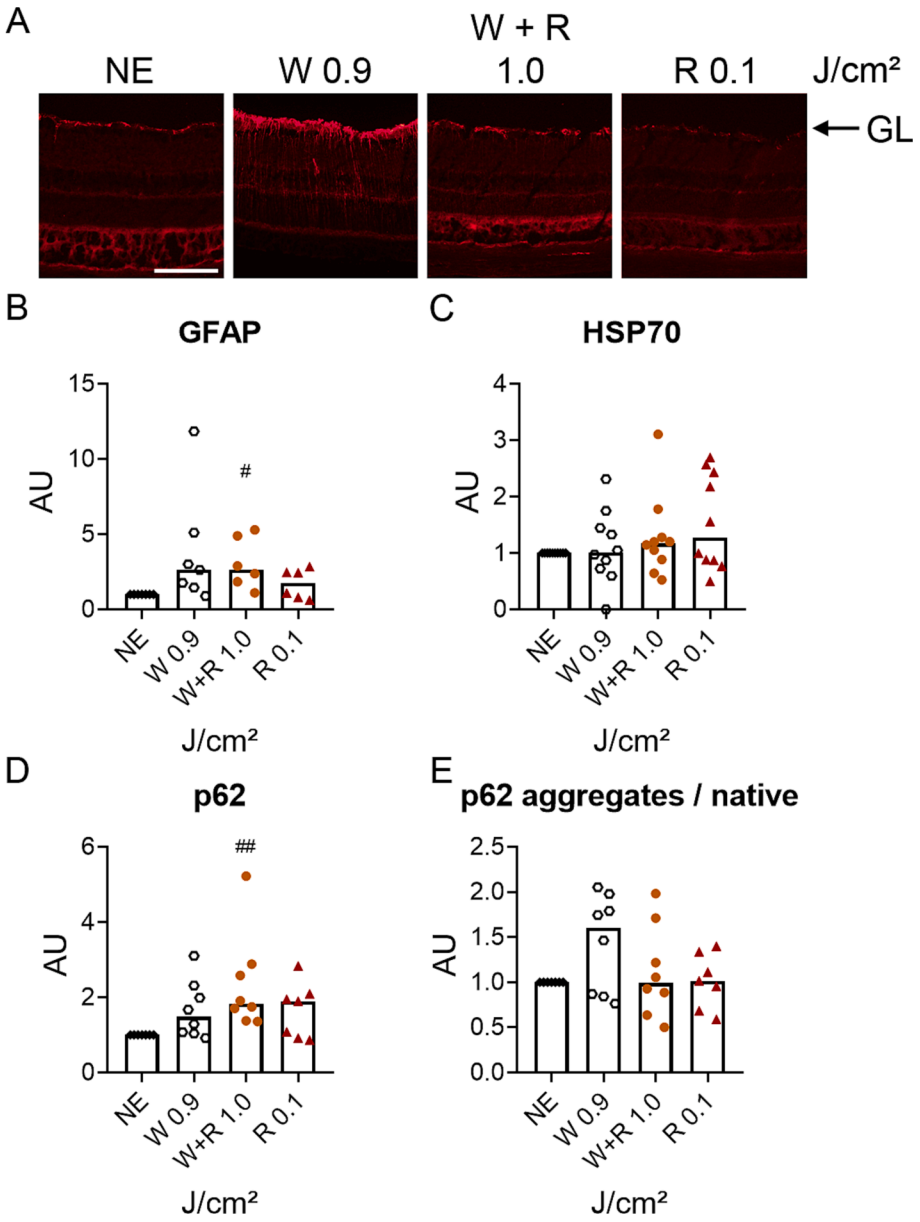


**Fig. 10. Effect of the red component in the cellular stress response of the retina.** A. Anti-GFAP immunolabeling on retina sections from rats exposed to white (W), red (R), or white and red LED simultaneously (W + R) or non-exposed (NE). GL: Ganglion Layer. Scale bar = 100 μm. B-E. Quantification by western blot of proteins involved in the stress response of the retina of rats exposed to white (W), red (R), or white and red LED simultaneously (W + R) or non-exposed (NE). B. $H(4) = 10.11$, $n \geq 6$ eyes. C. $H(4) = 1.203$, $n \geq 10$ eyes. D. $H(4) = 10.67$, $n \geq 7$ eyes. E. $H(4) = 1.880$, $n \geq 7$ eyes. Graphs represent the median. Statistical analysis was evaluated using the Kruskal-Wallis test followed by Dunn's post-tests. #: significance of the difference compared to NE, $\#p < 0.05$, $\#\#p < 0.01$. The addition of red light to white light did not significantly change the response of stress markers GFAP and HSP70, but increased p62. (For interpretation of the references to colour in this figure legend, the reader is referred to the web version of this article.)

and senescent cell cultures (Gutsmann-Conrad et al., 1998; Heydari et al., 1993). Since light is known to be one of the factors that trigger aging in the retina (Escobedo et al., 2022), downregulation of HSP70 protein after light exposure could be a sign of early aging induced by LED. Interestingly, upregulation of HSP70 expression has already been found in photobiomodulation (Evangelista et al., 2021). These authors show that red light (630 nm) applied on the skin once a day for 7 days at a dose of 9 J/cm$^2$ increases HSP70 protein level in a model of Achilles tendinitis in Wistar rats. We did not find this response after exposure to red light but this discrepancy could be attributed to the low retinal dose used in our study (0.1 J/cm$^2$).

Concerning p62/SQSTM1, the increase of its aggregates may promote autophagosome biogenesis indicating an attempt of the cell to maintain viability in stress conditions (Carroll et al., 2018). This phenomenon has already been shown in response to UV exposure (Zhao et al., 2013). Our results suggest that visible light at low doses also induces an increase in p62 aggregation (Figs. 6, 8, 10). This may indicate a potential effect of blue and white light on the autophagic pathway in the retina. This modulation could also corroborate the results found on the RPE layer, where light exposure induces an accumulation of rhodopsin aggregates that might be a sign of a failure of the RPE in its recycling function. Further studies are needed to precisely assess the effects of light exposure on autophagy and phagocytosis.

Red light therapy has been shown to reduce the inflammation in the context of aging and AMD (Begum et al., 2013; Kokkinopoulos et al., 2013), but also the inflammation caused by white fluorescent tubes (Albarracin et al., 2011). Our results suggest a protective effect of red against cell death but not against microglial invasion of the retina. This

is partially in accordance with the study of Nie et al., 2022, in which the authors created a low BLH LED by adding green and red LED to a phosphor white LED while keeping the same chromaticity (Nie et al., 2022). The difference found between studies may be due to the differences of the global light spectra used in both studies.

In light safety standards, the setup of phototoxicity thresholds relies on retinal degeneration. The activation of stress markers, in the absence of photoreceptor cell death, are not considered phototoxic. However, the repetitive induction of a stress response in the context of a chronic exposure could trigger further damage, including potential cell death.

### 4.4. Phototoxicity of low light doses on the RPE

The study of the impact of light exposure on the RPE shows that low doses of both blue and white light induce an alteration of the actin cytoskeleton indicating a potential loss of integrity of the outer blood-retinal barrier (OBRB). These alterations include ripples of the actin cytoskeleton for blue and white light and openings of the actin cytoskeleton from a retinal dose of 0.09 J/cm$^2$ BLH for white light (Figs. 2 and 4). Albumin leakage observed for the highest doses confirm the loss of integrity of the OBRB. These results are in accordance with the results obtained after the exposure to higher doses of light (from 4.14 J/cm$^2$), that highlight a worsening of the damage induced by light in a dose-dependent manner, eventually leading to the activation of necrosis in the RPE cells (Jaadane et al., 2017).

The global organization of the epithelium is also modified after white light exposure, with the appearance of numerous multinucleated cells already observed in the RPE of aged mice or after exposure to an oxidative stress leading to a cytokinesis defect (Chen et al., 2016), suggesting an early aging of the RPE.

Finally, exposure to light at low doses, especially to white light, potentially alters the capacity of the RPE to recycle photoreceptor wastes (Fig. 5). The accumulation of rhodopsin aggregates observed in our results can arise from the accumulation of undigested photoreceptor segments following light exposure, leading to a saturation of the phagocytic and recycling functions of the RPE. If not resolved, the accumulation of oxidized products may increase the oxidative stress, contributing to the activation of the inflammatory response and cell death in the RPE and in the retina (Rózanowska and Sarna, 2005; Sparrow and Boulton, 2005). A long-term study would be interesting to decipher whether the RPE is capable of taking care of the rhodopsin aggregates or if these accumulate further.

Taken together our results show that doses of light below the current phototoxicity threshold induce significant damage of the RPE that impacts its structure and function.

### 4.5. Positioning of our results to different uses of light

As mentioned above, light equipped devices are used for the treatment of pathological conditions (neonatal jaundice, acne, psoriasis, circadian rhythm disruptions, seasonal depressive disorders, pain, etc). In these different applications the exposure of the retina is different. It ranges from a bright exposure in luminotherapy (about 10 000 lx) with a short time of exposure (0.5 to 2 h) delivering to the human eye 0.1 J/cm$^2$ for 1 h of exposure, to higher exposure in the apparatus for the treatment of skin conditions (25 J/cm$^2$ for blue light at 415 nm and 3.70 J/cm$^2$ for red light (633 nm)) (Watjanatepin et al., 2022). However, when used with the recommended eye protections, these radiations do not reach the eye.

Concerning the exposure to artificial light for domestic lighting, the situation is different. The intensity of the light is lesser but the time of exposure is longer. Moreover, most of the exposure to artificial light is done during the night, when the sensitivity of the retina to light damage is more important. Actually, in many vertebrate species, vision at night is favored by a strong rod cone coupling (Ribelayga et al., 2008), which leads to a higher sensitivity of the retina to light at night (about three to four fold for rats) (Organisciak et al., 2000; Vaughan et al., 2002). A major point in the evaluation of the eventual negative impact of artificial light to our retina is the calculation of light exposure. In its report of 2019 concerning new lighting technologies, the ANSES (French Agency for food administration) carried out measurements in real life conditions and concluded that artificial lighting adds up to 50 % of the phototoxic dose received from natural lighting. This ratio can be increased to 200 % if only cool LED are used. Screens are one of the biggest artificial contributors to exposure in the different scenarios (Report ANSES 2019).

### 4.6. Positioning of our results to standard regulations

The overestimation of the phototoxicity threshold is demonstrated here in a rat model. It is interesting to note that the susceptibility to excessive light increases with age, as it has been shown in various species such as flies (Song et al., 2022) and rats (Organisciak et al., 1998). Thus, a more complete evaluation of the phototoxicity threshold using older animals would be interesting to perform.

Although the admitted phototoxicity thresholds for rodents and for primates differ: 22 J/cm$^2$ at 445 nm for primates and 11 J/cm$^2$ for rodents (van Norren and Gorgels, 2011), the same methods were used to determine these values in both species suggesting that values calculated for primates might also be overestimated. Interestingly, this idea has also been reported by Hunter and colleagues, who observed RPE disruption in macaque eyes *in vivo* following exposure to a 568 nm light, below the American standard for the maximum permissible exposure. They highlighted a potential overestimation by a factor of 20 of the current safety standards in humans (Hunter et al., 2018, 2012).

## 5. Conclusion

In this paper we show that the blue and green part of the spectrum are responsible for retinal phototoxicity while the red part has some protective properties. This leads to the conclusion that, in order to efficiently protect the retina, the phototoxicity of a polychromatic light should include the entire spectrum, not only its content in blue light as it is generally admitted. Moreover, we show that the retinal dose of light inducing photodamage in rats is overestimated in the current literature.

Taken together, our results indicate that the current phototoxicity threshold for humans along with the current methods to determine the latter require a re-assessment. This is of particular importance since the commercial LED that are currently classified as safe for the retina could actually induce retinal damage if used daily at high luminance. In addition, we show that the entire spectrum influences the phototoxicity of a light source. It is important to note that the artificial domestic lighting is nowadays almost exclusively done by the LED technology and its high blue content and small red content, corresponding to the exact opposite of what we previously had when using incandescent bulbs, which were extremely rich in red wavelengths and poor in blue light. This means that our lighting environment has dramatically changed in the last few years with consequences for our retina (as studied in this paper), our circadian rhythm (Meléndez-Fernández et al., 2023), and for the flora and fauna (Falcón et al., 2020; Nash et al., 2019).

**Funding**

This work was supported by ANSES (agence nationale de sécurité sanitaire de l'alimentation, de l'environnement et du travail, France) contract 2022/EST/134 to AT.

**CRediT authorship contribution statement**

**Anaïs Françon:** Writing – review & editing, Writing – original draft, Investigation, Formal analysis. **Francine Behar-Cohen:** Writing – review & editing. **Alicia Torriglia:** Writing – review & editing, Writing – original draft, Supervision, Funding acquisition, Conceptualization.

## Declaration of competing interest

The authors declare that they have no known competing financial interests or personal relationships that could have appeared to influence the work reported in this paper.

## Data availability

Data will be made available on request.

## Acknowledgements

Authors express their gratitude to Julia Pardo and Laurent Jonet for cryosections, Gaëlle Choumager and Lucy Foucher for animal care. Pr. Sabine Chahory for helpful discussions. Authors also thank Dr. Emilie Picard for providing the spectrophotometer device, and Drs. Christophe Martinsons, Samuel Carré, and Pierre Boulenguez from the Centre Scientifique et Technique du Bâtiment (CSTB) for the conception of the lighting device and the calculation software.

## Appendix A. Supplementary data

Supplementary data to this article can be found online at https://doi.org/10.1016/j.envint.2024.108471.

## References

Albarracin, R., Eells, J., Valter, K., 2011. Photobiomodulation protects the retina from light-induced photoreceptor degeneration. Invest. Ophthalmol. vis. Sci. 52, 3582. https://doi.org/10.1167/iovs.10-6664.

Begum, R., Powner, M.B., Hudson, N., Hogg, C., Jeffery, G., 2013. Treatment with 670 nm light up regulates cytochrome C Oxidase expression and reduces inflammation in an age-related macular degeneration model. PLoS ONE 8, e57828.

Benedetto, M.M., Contin, M.A., 2019. Oxidative stress in retinal degeneration promoted by constant LED Light. Front. Cell. Neurosci. 13, 139. https://doi.org/10.3389/fncel.2019.00139.

Brown, T.M., 2020. Melanopic illuminance defines the magnitude of human circadian light responses under a wide range of conditions. J Pineal Res 69, e12655.

Bullough, J.D., Bierman, A., Rea, M.S., 2019. Evaluating the blue-light hazard from solid state lighting. International Journal of Occupational Safety and Ergonomics 25, 311–320. https://doi.org/10.1080/10803548.2017.1375172.

Carroll, B., Otten, E.G., Manni, D., Stefanatos, R., Menzies, F.M., Smith, G.R., Jurk, D., Kenneth, N., Wilkinson, S., Passos, J.F., Attems, J., Veal, E.A., Teyssou, E., Seilhean, D., Millecamps, S., Eskelinen, E.-L., Bronowska, A.K., Rubinsztein, D.C., Sanz, A., Korolchuk, V.I., 2018. Oxidation of SQSTM1/p62 mediates the link between redox state and protein homeostasis. Nat Commun 9, 256. https://doi.org/10.1038/s41467-017-02746-z.

Chen, M., Rajapakse, D., Fraczek, M., Luo, C., Forrester, J.V., Xu, H., 2016. Retinal pigment epithelial cell multinucleation in the aging eye – a mechanism to repair damage and maintain homoeostasis. Aging Cell 15, 436–445. https://doi.org/10.1111/acel.12447.

Choi, J.-R., Shin, K.S., Choi, C.Y., Kang, S.J., 2016. PARP1 regulates the protein stability and proapoptotic function of HIPK2. Cell Death Dis 7, e2438.

Contín, M.A., Benedetto, M.M., Quinteros-Quintana, M.L., Guido, M.E., 2016. Light pollution: the possible consequences of excessive illumination on retina. Eye 30, 255–263. https://doi.org/10.1038/eye.2015.221.

L. Court Light and Visible Radiation A. Perrin M. Souques Electromagnetic Fields, Environment and Health 2012 Springer Paris Paris 97 108 10.1007/978-2-8178-0363-0_9.

Escobedo, S.E., Stanhope, S.C., Dong, Z., Weake, V.M., 2022. Aging and light stress result in overlapping and unique gene expression changes in photoreceptors. Genes 13, 264. https://doi.org/10.3390/genes13020264.

Evangelista, A.N., dos Santos, F.F., de Oliveira Martins, L.P., Gaiad, T.P., Machado, A.S. D., Rocha-Vieira, E., Costa, K.B., Santos, A.P., Oliveira, M.X., 2021. Photobiomodulation therapy on expression of HSP70 protein and tissue repair in experimental acute Achilles tendinitis. Lasers Med Sci 36, 1201–1208. https://doi.org/10.1007/s10103-020-03155-3.

Falcón, J., Torriglia, A., Attia, D., Viénot, F., Gronfier, C., Behar-Cohen, F., Martinsons, C., Hicks, D., 2020. Exposure to artificial light at night and the consequences for flora, fauna, and ecosystems. Front Neurosci 14, 602796. https://doi.org/10.3389/fnins.2020.602796.

Feng, J.-H., Dong, X.-W., Yu, H.-L., Shen, W., Lv, X.-Y., Wang, R., Cheng, X.-X., Xiong, F., Hu, X.-L., Wang, H., 2021. Cynaroside protects the blue light-induced retinal degeneration through alleviating apoptosis and inducing autophagy in vitro and in vivo. Phytomedicine 88, 153604. https://doi.org/10.1016/j.phymed.2021.153604.

Françon, A., Torriglia, A., 2023. Cell death mechanisms in retinal phototoxicity. Journal of Photochemistry and Photobiology 15, 100185. https://doi.org/10.1016/j.jpap.2023.100185.

Gorgels, T.G., van Norren, D., 1995. Ultraviolet and green light cause different types of damage in rat retina. Invest Ophthalmol vis Sci 36, 851–863.

Gorgels, T.G., Van Norren, D., 1998. Two spectral types of retinal light damage occur in albino as well as in pigmented rat: no essential role for melanin. Exp Eye Res 66, 155–162. https://doi.org/10.1006/exer.1997.0416.

Gosling, D.B., O'Hagan, J.B., Quhill, F.M., 2016. Blue laser induced retinal injury in a commercial pilot at 1300 ft. Aerospace Medicine and Human Performance 87, 69–70. https://doi.org/10.3357/AMHP.4411.2016.

Gutsmann-Conrad, A., Heydari, A.R., You, S., Richardson, A., 1998. The expression of heat shock protein 70 decreases with cellular senescencein vitroand in cells derived from young and old human subjects. Experimental Cell Research 241, 404–413. https://doi.org/10.1006/excr.1998.4069.

Ham, W.T., Mueller, H.A., Ruffolo, J.J., Guerry, D., Guerry, R.K., 1982. Action spectrum for retinal injury from near-ultraviolet radiation in the aphakic monkey. Am J Ophthalmol 93, 299–306. https://doi.org/10.1016/0002-9394(82)90529-3.

Hatori, M., Gronfier, C., Van Gelder, R.N., Bernstein, P.S., Carreras, J., Panda, S., Marks, F., Sliney, D., Hunt, C.E., Hirota, T., Furukawa, T., Tsubota, K., 2017. Global rise of potential health hazards caused by blue light-induced circadian disruption in modern aging societies. NPJ Aging Mech Dis 3, 9. https://doi.org/10.1038/s41514-017-0010-2.

Heinig, N., Schumann, U., Calzia, D., Panfoli, I., Ader, M., Schmidt, M.H.H., Funk, R.H. W., Roehlecke, C., 2020. Photobiomodulation mediates neuroprotection against blue light induced retinal photoreceptor degeneration. International Journal of Molecular Sciences 21, 2370. https://doi.org/10.3390/ijms21072370.

Heydari, A.R., Wu, B., Takahashi, R., Strong, R., Richardson, A., 1993. Expression of heat shock protein 70 is altered by age and diet at the level of transcription. Mol Cell Biol 13, 2909–2918.

Hu, Z., Zhang, Y., Wang, J., Mao, P., Lv, X., Yuan, S., Huang, Z., Ding, Y., Xie, P., Liu, Q., 2016. Knockout of Ccr2 alleviates photoreceptor cell death in rodent retina exposed to chronic blue light. Cell Death Dis 7, e2468–e. https://doi.org/10.1038/cddis.2016.363.

Hunter, J.J., Morgan, J.I.W., Merigan, W.H., Sliney, D.H., Sparrow, J.R., Williams, D.R., 2012. The susceptibility of the retina to photochemical damage from visible light. Prog Retin Eye Res 31, 28–42. https://doi.org/10.1016/j.preteyeres.2011.11.001.

Hunter, J.J., Morgan, J.I.W., Merigan, W.H., Williams, D.R., 2018. Retinal phototoxicity observed using high-resolution autofluorescence imaging. International Laser Safety Conference 2009, 61. https://doi.org/10.2351/1.5056723.

International Commission on Non-Ionizing Radiation Protection ICNIRP Guidelines on Limits of Exposure to Incoherent Visible and Infrared Radiation Health Physics 105 2013 74 96 10.1097/HP.0b013e318289a611.

Jaadane, I., Boulenguez, P., Chahory, S., Carré, S., Savoldelli, M., Jonet, L., Behar-Cohen, F., Martinsons, C., Torriglia, A., 2015. Retinal damage induced by commercial light emitting diodes (LEDs). Free Radic Biol Med 84, 373–384. https://doi.org/10.1016/j.freeradbiomed.2015.03.034.

Jaadane, I., Villalpando Rodriguez, G.E., Boulenguez, P., Chahory, S., Carré, S., Savoldelli, M., Jonet, L., Behar-Cohen, F., Martinsons, C., Torriglia, A., 2017. Effects of white light-emitting diode (LED) exposure on retinal pigment epithelium in vivo. J. Cell. Mol. Med. 21, 3453–3466. https://doi.org/10.1111/jcmm.13255.

Jaadane, I., Villalpando Rodriguez, G., Boulenguez, P., Carré, S., Dassieni, I., Lebon, C., Chahory, S., Behar-Cohen, F., Martinsons, C., Torriglia, A., 2020. Retinal phototoxicity and the evaluation of the blue light hazard of a new solid-state lighting technology. Sci Rep 10, 6733. https://doi.org/10.1038/s41598-020-63442-5.

Kim, Y.J., Kim, H.-J., Kim, H.L., Kim, H.J., Kim, H.S., Lee, T.R., Shin, D.W., Seo, Y.R., 2017. A protective mechanism of visible red light in normal human dermal fibroblasts: enhancement of GADD45A-mediated DNA repair activity. J Invest Dermatol 137, 466–474. https://doi.org/10.1016/j.jid.2016.07.041.

Kim, J., Won, J.Y., 2022. Effect of photobiomodulation in suppression of oxidative stress on retinal pigment epithelium. International Journal of Molecular Sciences 23, 6413. https://doi.org/10.3390/ijms23126413.

Kokkinopoulos, I., Colman, A., Hogg, C., Heckenlively, J., Jeffery, G., 2013. Age-related retinal inflammation is reduced by 670 nm light via increased mitochondrial membrane potential. Neurobiology of Aging 34, 602–609. https://doi.org/10.1016/j.neurobiolaging.2012.04.014.

Kotoglou, P., Kalaitzakis, A., Vezyraki, P., Tzavaras, T., Michalis, L.K., Dantzer, F., Jung, J.U., Angelidis, C., 2009. Hsp70 translocates to the nuclei and nucleoli, binds to XRCC1 and PARP-1, and protects HeLa cells from single-strand DNA breaks. Cell Stress Chaperones 14, 391–406. https://doi.org/10.1007/s12192-008-0093-6.

Lebon, C., Rodriguez, G.V., Zaoui, I.E., Jaadane, I., Behar-Cohen, F., Torriglia, A., 2015. On the use of an appropriate TdT-mediated dUTP-biotin nick end labeling assay to identify apoptotic cells. Anal Biochem 480, 37–41. https://doi.org/10.1016/j.ab.2015.04.007.

Legierski, M., Michałek, P., 2018. Assessment of photobiological safety of passing beam and driving beam headlamps with different light sources. IOP Conf. Ser.: Mater. Sci. Eng. 421, 032016 https://doi.org/10.1088/1757-899X/421/3/032016.

Liang, L., Cui, Z., Lu, C., Hao, Q., Zheng, Y., 2017. Damage to the macula associated with LED-derived blue laser exposure: a case report. BMC Ophthalmol 17, 49. https://doi.org/10.1186/s12886-017-0448-9.

Meléndez-Fernández, O.H., Liu, J.A., Nelson, R.J., 2023. Circadian rhythms disrupted by light at night and mistimed food intake alter hormonal rhythms and metabolism. Int J Mol Sci 24, 3392. https://doi.org/10.3390/ijms24043392.

Moradi-Marjaneh, R., Paseban, M., Moradi Marjaneh, M., 2019. Hsp70 inhibitors: implications for the treatment of colorectal cancer. IUBMB Life 71, 1834–1845. https://doi.org/10.1002/iub.2157.

Mtanes, K., Mimouni, M., Zayit-Soudry, S., 2018. Laser pointer-induced maculopathy: more than meets the eye. J Pediatr Ophthalmol Strabismus 55, 312–318. https://doi.org/10.3928/01913913-20180405-01.

Nash, T.R., Chow, E.S., Law, A.D., Fu, S.D., Fuszara, E., Bilska, A., Bebas, P., Kretzschmar, D., Giebultowicz, J.M., 2019. Daily blue-light exposure shortens lifespan and causes brain neurodegeneration in Drosophila. Npj Aging Mech Dis 5, 1–8. https://doi.org/10.1038/s41514-019-0038-6.

Naylor, A., Hopkins, A., Hudson, N., Campbell, M., 2019. Tight junctions of the outer blood retina barrier. Int J Mol Sci 21, 211. https://doi.org/10.3390/ijms21010211.

Nie, J., Xu, N., Chen, Z., Huang, L., Jiao, F., Chen, Y., Pan, Z., Deng, C., Zhang, H., Dong, B., Li, J., Tao, T., Kang, X., Chen, W., Wang, Q., Tong, Y., Zhao, M., Zhang, G., Shen, B., 2022. More light components and less light damage on rats' eyes: evidence for the photobiomodulation and spectral opponency. Photochem Photobiol Sci. https://doi.org/10.1007/s43630-022-00354-5.

Noell, W.K., Walker, V.S., Kang, B.S., Berman, S., 1966. Retinal damage by light in rats. Invest Ophthalmol 5, 450–473.

Oddone, E., Taino, G., Vita, S., Schimd, M., Frigerio, F., Imbriani, M., 2019. Macular degeneration: peculiar sunlight exposure in an agricultural worker. Med Lav 110, 241–245.

Organisciak, D.T., Darrow, R.M., Barsalou, L., Darrow, R.A., Kutty, R.K., Kutty, G., Wiggert, B., 1998. Light history and age-related changes in retinal light damage. Invest Ophthalmol vis Sci 39, 1107–1116.

Organisciak, D.T., Darrow, R.M., Barsalou, L., Kutty, R.K., Wiggert, B., 2000. Circadian-dependent retinal light damage in rats. Invest Ophthalmol vis Sci 41, 3694–3701.

Remé, C.E., Grimm, C., Hafezi, F., Wenzel, A., Williams, T.P., 2000. Apoptosis in the retina: the silent death of vision. News Physiol Sci 15, 120–124. https://doi.org/10.1152/physiologyonline.2000.15.3.120.

Ribelayga, C., Cao, Y., Mangel, S.C., 2008. The Circadian clock in the retina controls rod-cone coupling. Neuron 59, 790–801. https://doi.org/10.1016/j.neuron.2008.07.017.

Rózanowska, M., Sarna, T., 2005. Light-induced damage to the retina: role of rhodopsin chromophore revisited. Photochem Photobiol 81, 1305–1330. https://doi.org/10.1562/2004-11-13-IR-371.

Schick, T., Ersoy, L., Lechanteur, Y.T.E., Saksens, N.T.M., Hoyng, C.B., den Hollander, A. I., Kirchhof, B., Fauser, S., 2016. History of sunlight exposure is a risk factor for age-related macular degeneration. RETINA 36, 787. https://doi.org/10.1097/IAE.0000000000000756.

Shang, Y.-M., Wang, G.-S., Sliney, D., Yang, C.-H., Lee, L.-L., 2014. White Light-Emitting Diodes (LEDs) at domestic lighting levels and retinal injury in a rat model. Environ Health Perspect 122, 269–276. https://doi.org/10.1289/ehp.1307294.

Song, Y., Yang, J., Law, A.D., Hendrix, D.A., Kretzschmar, D., Robinson, M., Giebultowicz, J.M., 2022. Age-dependent effects of blue light exposure on lifespan, neurodegeneration, and mitochondria physiology in Drosophila melanogaster. npj Aging 8, 1–9. https://doi.org/10.1038/s41514-022-00092-z.

Sparrow, J.R., Boulton, M., 2005. RPE lipofuscin and its role in retinal pathobiology. Exp Eye Res 80, 595–606. https://doi.org/10.1016/j.exer.2005.01.007.

Sui, G.-Y., Liu, G.-C., Liu, G.-Y., Gao, Y.-Y., Deng, Y., Wang, W.-Y., Tong, S.-H., Wang, L., 2013. Is sunlight exposure a risk factor for age-related macular degeneration? a systematic review and meta-analysis. Br J Ophthalmol 97, 389–394. https://doi.org/10.1136/bjophthalmol-2012-302281.

Tang, W., Guo, J., Liu, W., Ma, J., Xu, G., 2021. Ferrostatin-1 attenuates ferroptosis and protects the retina against light-induced retinal degeneration. Biochemical and Biophysical Research Communications 548, 27–34. https://doi.org/10.1016/j.bbrc.2021.02.055.

Torp-Pedersen, T., Welinder, L., Justesen, B., Christensen, U.C., Solborg Bjerrum, S., La Cour, M., Saunte, J.P., 2018. Laser pointer maculopathy - on the rise? Acta Ophthalmol 96, 749–754. https://doi.org/10.1111/aos.13856.

Torriglia, A., Jaadane, I., Lebon, C., 2016. Mechanisms of cell death in neurodegenerative and retinal diseases: common pathway? Current Opinion in Neurology 29, 55–60. https://doi.org/10.1097/WCO.0000000000000272.

van Norren, D., Gorgels, T.G.M.F., 2011. The action spectrum of photochemical damage to the retina: a review of monochromatic threshold data. Photochemistry and Photobiology 87, 747–753. https://doi.org/10.1111/j.1751-1097.2011.00921.x.

Vaughan, D.K., Nemke, J.L., Fliesler, S.J., Darrow, R.M., Organisciak, D.T., 2002. Evidence for a circadian rhythm of susceptibility to retinal light damage. Photochem Photobiol 75, 547–553. https://doi.org/10.1562/0031-8655(2002)075<0547:efacro>2.0.co;2.

Watjanatepin, N., Kiatsookkanatorn, P., Boonmee, C., Thongkullaphat, S., Archevapanich, T., Sritanauthaikorn, P., Wannakam, K., 2022. Design and realization of a dual-wavelength low level light therapy for acne and face rejuvenation treatment. IJEECS 29, 147. https://doi.org/10.11591/ijeecs.v29.i1.pp147-160.

Wu, J., Seregard, S., Algvere, P.V., 2006. Photochemical Damage of the Retina. Survey of Ophthalmology 51, 461–481. https://doi.org/10.1016/j.survophthal.2006.06.009.

Zhao, Y., Zhang, C.-F., Rossiter, H., Eckhart, L., König, U., Karner, S., Mildner, M., Bochkov, V.N., Tschachler, E., Gruber, F., 2013. Autophagy is induced by UVA and promotes removal of oxidized phospholipids and protein aggregates in epidermal keratinocytes. Journal of Investigative Dermatology 133, 1629–1637. https://doi.org/10.1038/jid.2013.26.

Zhou, H., Zhang, H., Yu, A., Xie, J., 2018. Association between sunlight exposure and risk of age-related macular degeneration: a meta-analysis. BMC Ophthalmol 18, 331. https://doi.org/10.1186/s12886-018-1004-y.

Zhuang, X., Ma, J., Xu, S., Zhang, M., Xu, G., Sun, Z., 2021. All-trans retinoic acid attenuates blue light-induced apoptosis of retinal photoreceptors by upregulating MKP-1 expression. Mol Neurobiol 58, 4157–4168. https://doi.org/10.1007/s12035-021-02380-3.